Electrochemical methanation of carbon dioxide: Advances, challenges, and perspectives for biogas upgrading

Renewable and Sustainable Energy Reviews 226 (2026) 116365

Contents lists available at ScienceDirect

Renewable and Sustainable Energy Reviews

journal homepage: www.elsevier.com/locate/rser

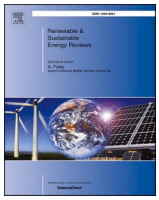

Electrochemical methanation of carbon dioxide: Advances, challenges, and perspectives for biogas upgrading

Sara Verhovez [a,b,*], Alexandru Morosanu [c], Adriano Sacco [a]

[a] Istituto Italiano di Tecnologia, Center for Sustainable Future Technologies @Polito, Via Livorno 60, 10144, Torino, Italy
[b] Politecnico di Torino, Department of Applied Science and Technology, Corso Duca degli Abruzzi 24, 10129, Torino, Italy
[c] Hysytech S.r.l., Via I° Maggio 5, 10043, Orbassano, TO, Italy

ARTICLE INFO

Keywords:
Electrochemical CO_2 reduction reaction
Methanation
Biogas
Technoeconomic analysis
Electrocatalyst
Reactor

ABSTRACT

The electrochemical conversion of carbon dioxide to methane is emerging as promising strategy for both mitigating CO_2 emissions and enabling renewable energy storage in a chemically stable, energy-dense form. Among the possible products of CO_2 electroreduction, methane stands out due to its high volumetric energy density, compatibility with existing natural gas infrastructure, and potential for direct integration into current energy systems. This review provides a comprehensive overview of the recent advancements in the electrochemical CO_2-to-CH_4 conversion, with particular focus on catalyst development, cell configurations, and system-level performance under industrially relevant conditions. Key challenges such as low selectivity, limited current densities and long-term operational stability are critically discussed. In addition, the review also explores the techno-economic aspects of electrochemical methanation, highlighting pathways toward scalable and sustainable deployment. Special emphasis is then placed on the potential application of this technology for biogas upgrading, which offers a unique advantage by utilizing an already CO_2-rich feedstock without the need for additional separation steps. Finally, we outline future directions for research aimed at making electrochemical biogas upgrading a viable component of circular carbon and renewable energy strategies.

1. Introduction

Global warming is one of the most pressing challenges of our time, with profound implications for the environment, economy and society [1]. This phenomenon is mainly caused by increasing greenhouse gas (GHG) concentrations in the atmosphere, resulting from human activities such as fossil fuel burning, deforestation and industrialization. In fact, despite the greenhouse effect is natural and necessary to maintain temperatures compatible with life, excessive GHG emission in the last 50 years has intensified this process, leading to rising global temperatures. Consequences include melting glaciers, rising sea levels, extreme weather events, and alterations in ecosystems [2]. Carbon dioxide (CO_2) is the main GHG because it is the most abundant and has a long residence time in the atmosphere. In fact, although other gases have a greater impact in the short term, CO_2 is the main contributor to long-term global warming [3].

To address the increase in CO_2 emissions, Carbon Capture, Utilization and Storage (CCUS) technology has emerged. CCUS encompasses a range of processes to capture CO_2 emitted from air, industrial and power sources, use it in various ways, or store it in deep geological formations to prevent its release into the atmosphere [4]. CCUS is considered a crucial technology for achieving global climate goals, as it can reduce emissions in sectors that are difficult to decarbonize and remove CO_2 already in the atmosphere. However, its large-scale implementation still faces challenges related to high costs, the need for adequate infrastructure, and public acceptance. In this framework, the demand for alternative renewable and sustainable fuels alternative to fossil-based ones is continuously increasing [5].

In this framework, the electrochemical CO_2 reduction reaction (eCO_2RR) is gaining considerable attention due to its ability to convert CO_2 into energy-rich molecules using electricity, ideally derived from intermittent renewable sources such as wind and solar power [6]. This dual function of eCO_2RR, enabling both carbon mitigation and renewable energy storage, positions it as a promising route to address the twin challenges of decarbonization and energy transition. Compared to conventional CO_2 conversion methods, such as thermochemical, catalytic hydrogenation, or biological pathways, the electrochemical approach offers several distinct advantages [7]. Thermochemical processes, while

* Corresponding author. Istituto Italiano di Tecnologia, Center for Sustainable Future Technologies @Polito, Via Livorno 60, 10144, Torino, Italy.
E-mail address: sara.verhovez@polito.it (S. Verhovez).

https://doi.org/10.1016/j.rser.2025.116365
Received 31 July 2025; Received in revised form 30 September 2025; Accepted 6 October 2025
Available online 11 October 2025

mature and capable of high throughput, often require high temperatures and pressures, leading to significant energy input and, in many cases, dependence on hydrogen derived from fossil fuels [8]. Biological routes, including microbial electrosynthesis or enzymatic conversion, tend to operate under milder conditions but suffer from slower reaction rates, complex process control, and scalability limitations [9]. In contrast, eCO_2RR proceeds under ambient or near-ambient conditions, exhibiting high reproducibility and precise controllability, while also permitting the use of green chemical reagents and sustainable supporting electrolytes [10]. Furthermore, its modularity and scalability make it well-suited for decentralized applications, directly coupling with renewable electricity sources for on-demand chemicals synthesis [11].

Among the various products obtainable from the electrochemical reduction of CO_2, methane (CH_4) stands out as a particularly promising target due to its high volumetric energy density, ease of liquefaction, and full compatibility with existing natural gas infrastructure for storage, distribution, and utilization [12]. These features make CH_4 a strategic energy carrier, especially in regions with established gas networks or policies oriented toward the replacement of fossil-derived natural gas with renewable synthetic alternatives [13]. The electrochemical conversion of CO_2 to CH_4 thus emerges as a compelling approach for storing intermittent renewable energy in a stable chemical form, while simultaneously contributing to carbon recycling and the decarbonization of the energy sector. Advancing this technology requires a multidisciplinary effort focused on several key factors, including the design and development of electrocatalysts, optimized reactor configurations, and finely tuned operating conditions capable of ensuring efficiency, scalability, and long-term stability [14,15]. This development can also benefit from some technoeconomic analysis (TEA) feasibility work [16].

In this framework, given the growing interest in this technology and considering the many points yet to be resolved, there is room for a review that systematically investigates all aspects involved in the electrochemical conversion of CO_2 to CH_4. For this reason, the next sections will provide an introduction of eCO_2RR (section 2), a bibliometric analysis on scientific literature for CO_2-to-CH_4 conversion (section 3), details on reactors (section 4), catalysts (section 5) and operative conditions (section 6) used for this process, scaling up (section 7), and technoeconomic analysis (section 8). Finally, critically analyzing what presented in the review, in section 9 we look at an application scenario in which electrochemical conversion of CO_2 to CH_4 could be particularly successful, namely the biogas upgrading. We thus demonstrate that the future of electrochemical CO_2 methanation depends on the co-optimization of catalyst stability, reactor architecture, and operating parameters, as well as on the integration with biogas feeding strategies and with renewable energy sources capable of reducing the cost of electricity.

2. Electrochemical CO_2 reduction reaction

The electrochemical CO_2 reduction reaction is carried out in an electrolyzer cell, typically composed by the cathode (where eCO_2RR occurs), the anode (where a counter-reaction such as oxygen evolution takes place), and an ion exchange membrane separating the two compartments (that allows passage of ions to close the circuit). Under the application of an electrical current, electrons are transferred to CO_2 molecules at the cathode; this transfer is balanced by ion passage through the ion exchange membrane.

A great variety of reactions can be obtained with this process, each leading to the formation of specific products with varying reduction potentials. In addition to methane, the main end products that can be obtained are carbon monoxide (CO), formate ($HCOO^-$), ethylene (C_2H_4), and ethanol (C_2H_5OH), which are selected depending on choice of catalyst and reaction conditions. Indeed, the selectivity (*i.e.* the capability of convert CO_2 to a single product) and efficiency of this process are enhanced by the choice of catalyst employed on the cathode. As an example, metals such as silver (Ag) and gold (Au) are mostly selective for CO production, while copper (Cu) is unique in its ability to catalyze the formation of more complex hydrocarbons. The product selectivity is mainly determined by the binding strength between catalyst and adsorbed reaction intermediates such as *H, *COOH, *OCOH, and *CO. This affinity can be predicted using the Sabatier principle, graphically described in a volcano plot, which defines the optimum interaction strength between catalyst and reactant.

The formation of different products involves varying numbers of electron and proton transfers, which directly influences the overpotentials required to drive the reactions. In fact, the production of carbon monoxide (CO) and formate ($HCOO^-$) can be obtained with a relatively simple two-electron transfer, while the generation of hydrocarbons can require six to twelve electrons and associated proton transfers, leading to more complex reaction pathways with multiple intermediate steps which usually each involve one or two electrons. These multielectron processes typically demand significantly higher overpotentials to overcome kinetic barriers and stabilize intermediates, and also complicate the determination of product selectivity.

Many different figures of merit are used to define the performance of electrolyzers for eCO_2RR, such as Faradaic efficiency/selectivity, current density, cell overpotential, energetic efficiency, and stability. The Faradaic efficiency determines the amount of current used to convert to a specific product, effectively describing the selectivity of a reaction. It is generally defined as:

$$FE = \frac{z\,n\,F}{Q}$$

where z is the number of required electrons for the reaction, n represents the number of moles of the given product, F is Faraday's constant, and Q is the total charge exchanged during the process.

The current density is defined as the overall current divided by the active electrode area. It is a measure of the electrochemical reaction rate per area of electrode and is a key parameter for the scale up of this technology, as high current densities are needed for industrial viability. From this figure of merit, it is possible to define the partial current density, which simply refers to the current associated to the formation of a specific product, providing insight into catalytic activity and selectivity. It is obtained by multiplying the total current density by the Faradaic efficiency of the target product.

The cell overpotential, defined as:

$$\eta = E - E^0$$

represents the difference between the potential applied to the cell (E) and the equilibrium potential of the half reaction (E^0). It is also used to determine the energy efficiency (EE), which measures the amount of energy applied to the system that is actually stored and employed for the reaction toward a specific product. The energy efficiency of the system can be defined as:

$$EE = \frac{E^0}{E^0 + \eta} FE$$

Finally, the stability quantifies the amount of time over which the system can operate maintaining target performance.

While all these parameters are crucial for the development of an efficient system, the optimization of each one simultaneously remains a major challenge. In practice, efforts to improve one figure of merit often come at the expense of another, highlighting trade-offs and difficulties that must be addressed to make CO_2 electroreduction viable at industrial level. This aspect will be analyzed in details in Section 7.1. In particular, one of the main challenges in the electrochemical reduction of CO_2 is the competition with the hydrogen evolution reaction (HER) in aqueous electrolytes, as both processes can occur simultaneously at the cathode and are regulated by similar reaction potentials. In fact, the onset of HER can significantly reduce the efficiency of CO_2RR by employing electrons that could otherwise reduce CO_2. Consequently, catalysts and reaction

conditions should be carefully designed and optimized as to minimize HER and maximize eCO_2RR, thus improving the selectivity and reaction rate.

3. Bibliometric analysis

A brief bibliometric analysis was conducted in order to gain insights into the research trend and development of eCO_2RR towards methane in the time period between 2008 and 2024, to isolate and quantify the main aspects involved in the development of electrochemical technologies for methane production. The analysis was based on data retrieved from the Web of Science (WoS) database using a carefully constructed search query designed to capture relevant studies, which is reported below:

TS = “CO2 electroreduction”, OR TS = “Electroreduction of carbon dioxide”, OR TS = “CO2 electrochemical reduction”, OR TS = “Electrochemical reduction of carbon dioxide”, OR TS = “Electrocatalytic reduction of CO2”, OR TS = “Electrocatalytic reduction of carbon dioxide”, OR TS = “CO2RR”, OR TS = “eCO2RR" AND (TS = "towards CH4" OR TS = "to CH4" OR TS = "toward* methane" OR TS = "to methane")

An initial screening was performed by excluding topic areas that are not involved in the subject (such as *Mineralogy, Biochemistry, Acoustics, Mining Mineral Processing, Microbiology*). A second exclusion criterion was used to eliminate duplicated papers, conference papers, or book chapters and papers not published in English. Due to the large amount of papers containing overlapping terminology, additional keyword filters were added to the search query (“NOT thermocataly* AND NOT photocataly* AND NOT microbial AND NOT methanation”) in order to minimize retrieval of papers that discussed catalytic conversion in non-electrochemical contexts. In cases where publications mentioned electrocatalysis only tangentially or in unrelated frameworks, these were further excluded through manual screening of titles, abstracts, and keywords. Moreover, some additional sources were manually incorporated, employing a snowball method by looking into relevant publications on the reference lists of two review papers [17,18]. The final search yielded a total of 1714 documents. The refined dataset was then imported into VOSviewer [19] and Biblioshiny (a web interface for the *bibliometrix* package in R) [20] for in-depth analysis and data visualization.

The overall metadata and bibliometric indicators derived from the dataset are summarized in Fig. 1a. The results indicate a significant and growing interest in the eCO_2RR-to-methane research area. From 2008 to 2024, the field experienced a growth rate of 31.83 %, reflecting an increasing number of publications and active contributors, with 7345 unique authors identified.

Notably, the number of published papers along with the total citation count (as illustrated in Fig. 1b) demonstrates an almost exponential rise beginning in 2013. This suggests that eCO_2RR towards CH_4 is gaining interest considerably and evolving into a prominent subfield within the broader carbon dioxide utilization and renewable energy research domains.

Based on bibliometric data, publications related to the electrochemical reduction of CO_2 to methane are distributed across a variety of subject categories. Most papers are concentrated in areas such as *Chemistry*, *Chemistry Multidisciplinary*, and *Materials Science Multidisciplinary*, reflecting the focus on development of catalyst and process analysis. In addition to these primary categories, other significant areas of research include *Nanoscience Technology* and *Engineering Chemical,* highlighting how the field is moving toward more advanced materials (e.g. nanocatalysts) and optimization of process and experimental designs to make this process more efficient and practical.

Overall, the analysis suggests that this area is highly interdisciplinary, proving that the challenge of converting CO_2 into methane requires a broad, collaborative approach spanning across different areas of both fundamental and practical science. This observation is confirmed by a brief overview of the journals where the selected publications appeared, offering insight into the main disciplinary focuses of the field. A significant portion of the literature is published in journals dedicated to catalysis and electrocatalysis, highlighting the fundamental role of catalyst design and engineering. Many contributions also appear in outlets focused on emerging materials and molecular systems for energy and environmental applications, underlining the relevance of advanced functional materials. The presence of journals centered on electrochemistry and applied chemical engineering further confirms the highly interdisciplinary nature of this research area, which sits at the intersection of fundamental science and technological innovation.

To further understand the thematic focus and research priorities within the field, an analysis of abstract and title keywords was conducted, using VOSviewer for visualization of the results. Keywords offer valuable insight into the core topics, materials, and methodologies that define a research domain. In the resulting network map, reported in Fig. 2, dense clusters indicate strong thematic connections between terms, while larger and thicker nodes represent keywords found with higher frequency in the literature.

For this specific topic, the keyword analysis revealed six distinct clusters, each representing a thematic focus. Cluster 1 included keywords related to the *reaction pathway* to CH_4 (*CO conversion*, *HCOOH*, *electron transfer*) along with terms like *DFT*, *electronic structure* and *binding energy*, suggesting that gaining fundamental insight into the reaction pathway to methane formation is a key research focus. Similarly, cluster 2 mentions *local pH*, *copper surface* and *CO intermediate*, which are all critical factors or for methane formation. The interplay between clusters 1 and 2 illustrates a main focus in the literature, both on the

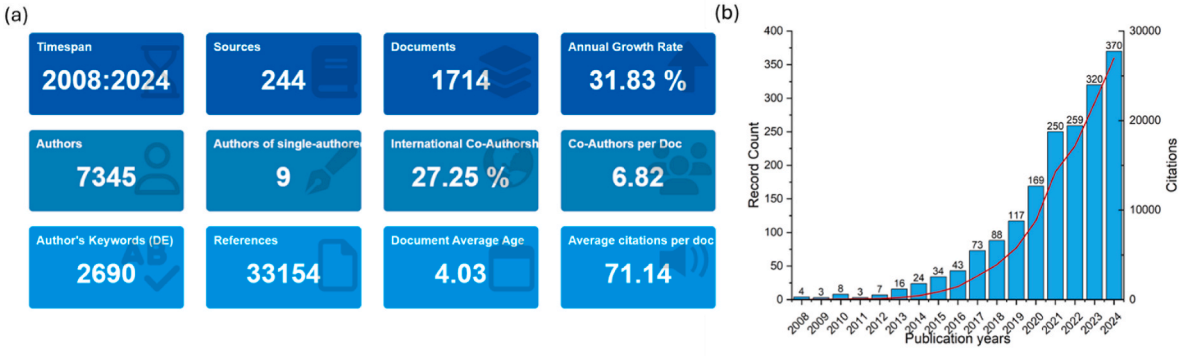

Fig. 1. (a) Overview of the main information about the target literature; (b) Number of publications (bars, left axis) for each year in the analyzed time period (2008–2024), along with the number of total citations (red line, right axis). (For interpretation of the references to colour in this figure legend, the reader is referred to the Web version of this article.)

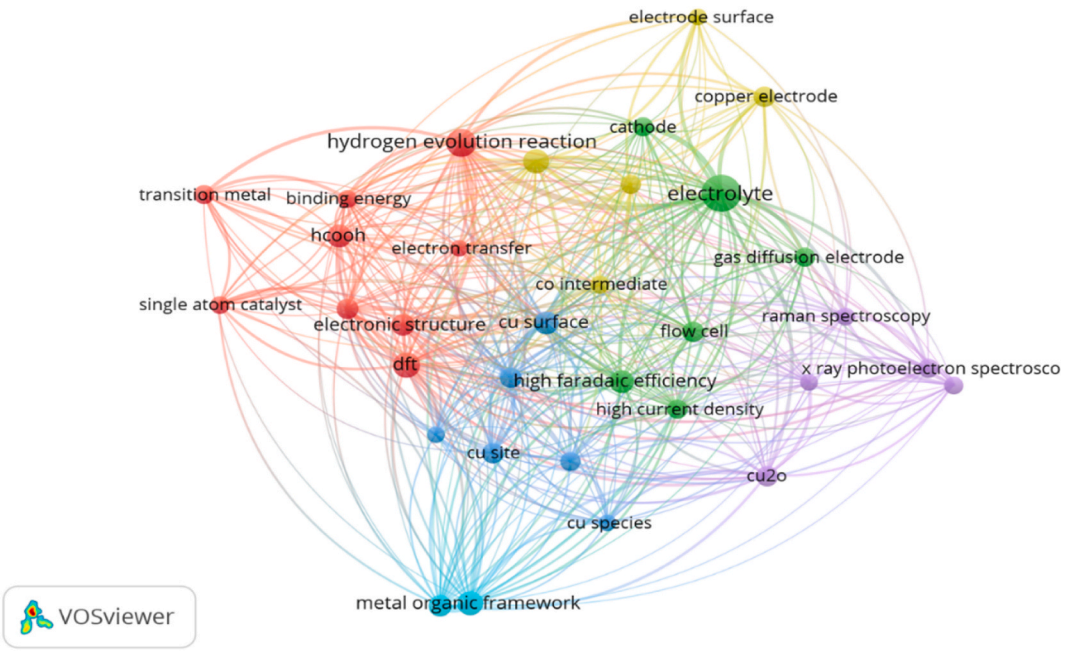

Fig. 2. Keywords network visualization for the electrochemical CO_2 conversion targeted to methane.

specific pathway conversion to methane, but also on interfacial conditions that modulate selectivity. The overlap between clusters suggests that progress in methane-selective CO_2 reduction requires simultaneous control of both catalyst structure and the reaction microenvironment.

Cluster 3 is mostly characterized by keywords associated with spectroscopic techniques, including *Raman spectroscopy* and *X-ray spectroscopy*, which frequently appear alongside terms like *Cu species* and *Cu_2O*. This indicates that these methods are commonly used to monitor copper oxidation states and behavior. Moreover, the high number of intersections with cluster 2 reinforce the notion that mechanistic understanding is increasingly being built upon *in situ* and *operando* measurements, which directly connect catalyst structure with interfacial phenomena. To support this claim, cluster 4 contains terms such as *Cu surface*, *active sites*, and *electronic structure*, further emphasizing the importance of catalyst characterization. Taken together with cluster 3, this cluster suggests that copper-centered studies dominate the field, reflecting its status as the benchmark material for CO_2-to-hydrocarbon conversion, but also highlighting a relative lack of diversification into non-copper systems. In cluster 5, words that are related to the cell design such as *GDE*, *flow cell*, *electrolyte* and *cathode* are shown, highlighting the main focal points for system design and optimization. Along with them are also words to describe performance such as *faradaic efficiency* and *high current density,* reflecting the importance of architecture and operative conditions optimization to achieve commercially viable performance of the system. Moreover, the high number of interconnections of this cluster with clusters 2 and 4 reveals the importance of operative system reaction conditions for stabilizing reaction intermediates and reach optimal performance. Finally, cluster 6 groups emerging materials and strategies such as *metal–organic frameworks* (MOFs) and *ionic liquids* that are appearing with growing frequency, indicating an evolving research direction. Interestingly, MOFs in particular exhibit strong interconnections with clusters 3 and 4, being linked with terms such as single-atom catalysts, Cu species, Cu sites, and Cu_2O. This indicates their role in catalyst engineering, as they are often employed in hybrid approaches to support atomically dispersed metals or stabilize copper oxidation states.

Overall, the six clusters demonstrate both the maturity and the evolving directions of the field. The literature is anchored in copper-based mechanistic and characterization studies (clusters 1–4), while parallel streams are advancing system-level optimization (cluster 5) and diversifying into novel material-focused strategies and directions (cluster 6). The strong overlaps between clusters highlight that future progress will likely depend on integrating insights across scales, from electronic structure to device design, rather than treating these domains in isolation. All these aspects will be analyzed in the following sections.

To complement the keyword clustering, a thematic map (Fig. 3) was generated in order to classify research themes according to their degree of development (density) and their overall relevance (centrality). This framework provides a deeper understanding of which topics are currently well-established, which are emerging, and which are driving the field forward.

Basic themes occupy the lower-right quadrant of the map, representing topics that are highly relevant but not necessarily the most innovative. In this field, keywords such as *carbon monoxide*, *copper electrode*, and *hydrogen evolution* dominate this category. Their positioning reflects their centrality to methane-selective CO_2 reduction: CO is the key intermediate in the methane pathway, copper remains the benchmark catalyst due to its unique ability to bind and transform CO intermediates, and hydrogen evolution persists as the most significant competing reaction, often favored under operational conditions that also promote methane formation. These themes form the conceptual foundation of the field, as they are universally studied and underpin almost all other research directions.

Emerging or declining themes appear in the lower-left quadrant. These topics exhibit low density and low centrality, meaning they are either underexplored areas of opportunity or subjects losing traction in the field.

Highly specialized or niche themes, in the upper-left quadrant, are well-developed but peripheral. They are characterized by high density (indicating focused, advanced study) yet low centrality (suggesting limited overall influence on the broader field). Examples include *active sites* and *graphene* in catalyst engineering. These areas often yield deep mechanistic insights or novel material strategies, but they remain relatively confined in scope. Their presence indicates that while specialized investigations are advancing, broader integration with mainstream research could unlock their impact. For instance, integrating graphene into catalyst engineering might bridge these niche efforts with central challenges in the field.

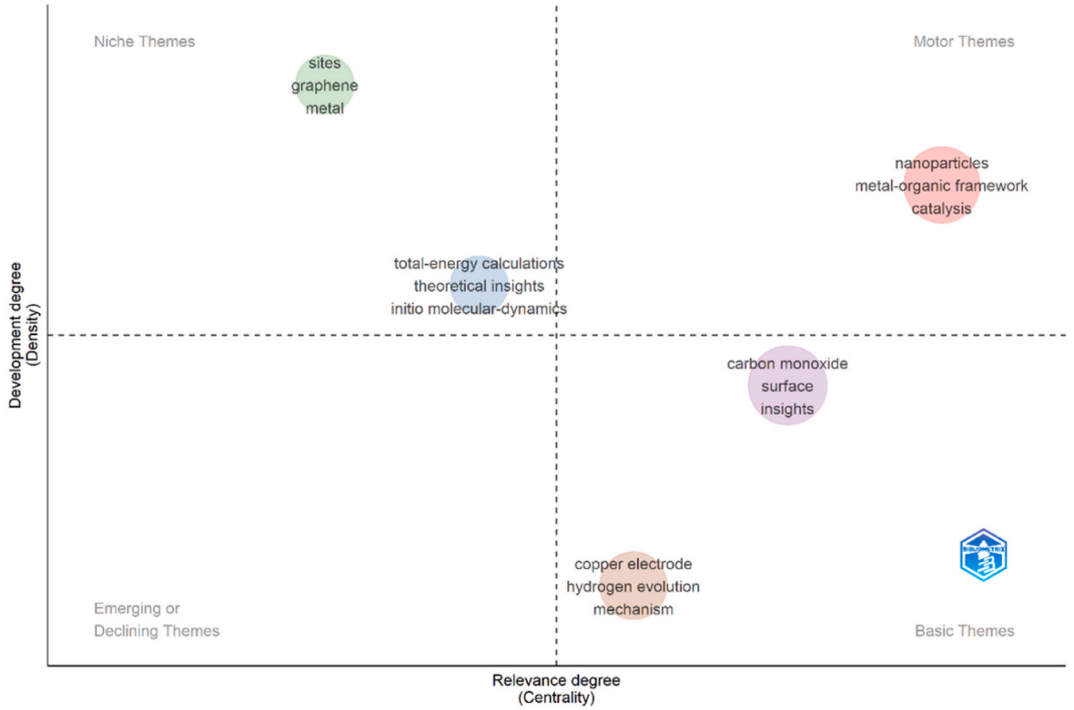

Fig. 3. Thematic map of key topics in the field of CO_2RR to methane, classified by their development and relevance degree into Niche, Motor, Emerging/Declining and Basic themes.

Finally, motor themes, located in the upper-right quadrant, are both highly developed and highly relevant, representing the main topics that are progressively moving forward the field. In this analysis, terms such as *nanoparticles, metal–organic frameworks (MOFs)*, and *catalysis* fall into this category. Their presence underscores the central role of catalyst engineering in advancing electrochemical conversion towards methane. The appearance of MOFs alongside nanoparticles reflects a trend towards hybrid or structurally tunable catalysts; together with the recurring theme of *catalysis*, this highlights the great need to focus on catalyst engineering and design in order to improve activity and selectivity.

4. Reactors

As anticipated, the system design and operational parameters impact several key factors of eCO_2RR, such as the cell overpotential, mass transport, stability, reaction rates and product selectivity. Each electrolyzer design has several variations which come with trade-offs across the various metrics that define their performance, which may pose some limitations to the development of scaled up systems for industrial applications. As the electrochemical conversion of CO_2 to CH_4 particularly requires precise control over a multi-step eight-electrons transfer reaction, the choice of cell architecture must balance fundamental mechanistic insights with practical considerations like scalability and energy efficiency.

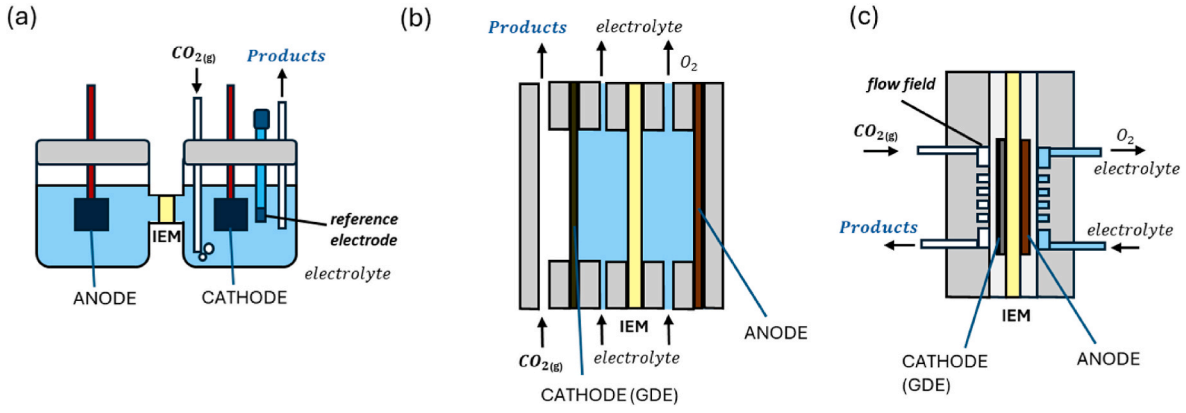

Fig. 4. Schematic comparison of three representative electrochemical cell configurations for CO_2 reduction. The H-cell (a) consists of two electrolyte chambers in which the electrodes are immersed, separated by an ion-exchange membrane, with CO_2 bubbled into the catholyte; it is useful for mechanistic studies but limited by CO_2 solubility and low current densities. The flow cell design (b) still features two electrolyte chambers on both anode and cathode side, along with a gas chamber directly behind the cathode. Moreover, the introduction of GDEs at the cathode side enables direct CO_2 supply from behind the GDE, while a liquid electrolyte flows on the other side of the electrode, improving mass transport but introducing challenges such as electrode flooding. In the MEA or zero-gap configuration (c), while the gas is again delivered directly behind the GDE through a serpentine flow-field, the catalyst layer is in direct contact with the ion-exchange membrane, eliminating bulk liquid electrolyte on the cathode side and maintaining an electrolyte chamber only on the anode side.

H-type cells, sketched in Fig. 4a, are one of the most commonly used reactor configurations in fundamental studies of electrochemical CO_2 reduction at laboratory scale. Structurally, an H-cell consists of two compartments—anodic and cathodic—separated by an ion-conducting membrane, allowing selective ion transfer while also preventing product crossover. CO_2 is pumped continuously on the cathodic side, where the electrochemical reduction reaction occurs. This setup allows precise control over experimental conditions, making it highly suitable for mechanistic studies, analysis of reaction pathways and catalyst behaviour. H-type cells are widely used in the field for catalyst studies: different works reached notably high selectivity (50 %–86 %) towards methane [21–26], but always maintaining current density below 10 mA/cm^2. In fact, although the physical separation enables high product selectivity and low product crossover, a key limitation of this setup still remains: the reactions are mass-transport limited, primarily due to the low solubility and slow diffusion of CO_2 in aqueous electrolytes, which strongly hinders the reaction rates and limits its application at industrial level.

A flow cell system, as shown in Fig. 4b, provides an effective strategy to overcome this crucial limitation by introducing the gas diffusion electrode (GDE), a gas–liquid–solid triple-phase interface, which allows direct CO_2 delivery to the catalyst active sites, thus supporting the high CO_2 flux necessary to reach increased current density. In fact, within this configuration, CO_2 is supplied directly from a gas chamber situated behind the GDE while a liquid electrolyte flows past the catalyst layer on the opposite side of the GDE, ensuring both ion transport and product removal. This arrangement decouples CO_2 delivery from its limited solubility in aqueous media and enables operation at industrially relevant current densities, but at the cost of introducing new operational complexities. This change in system setup, and therefore in experimental conditions, pH and reaction rate, results in a significantly different product distribution from that observed in conventional H-cell configurations. While the separation of the CO_2 gas from the electrolyte allows the use of highly alkaline solutions, which have better ionic conductivity and therefore low voltage loss, an alkaline pH in the cell has been found to promote C_{2+} products formation, reducing current density and selectivity towards methane [27]. Therefore, achieving a high Faradaic efficiency for CH_4 at high current densities with this setup still poses a challenge, also due to competing reactions such as HER. Rasouli et al. were able to directly translate a H-cell system to a flow cell based one by modelling the local pH and matching it to the one corresponding to highest H-cell methane FE [28], successfully overcoming the current density limit. Many other works employing flow cells were able to reach high FE while maintaining technoeconomical compelling current densities [29–33]. However, the main limitation encountered in this system is the inevitable flooding of the GDE despite its excellent stability, which typically happens within several hours of operation [34]. This phenomenon involves the intrusion of bulk electrolyte into the GDE, which causes blockage of pores and prevents CO_2 from reaching active sites, resulting in a decrease of eCO_2RR products in favor of HER and ultimately driving the system to critical failure [35]. There are different factors that contribute to this phenomenon, such as electrowetting (where the applied potential alters the superficial tension of the GDE, increasing water penetration into the layers), pressure imbalances between the gas and liquid phases at the interface, salt precipitation and accumulation on the surface [36].

More recently, membrane electrode assemblies (MEAs) have emerged as a very promising configuration, due to their potential to overcome technical difficulties and limitations of eCO_2RR. As shown in Fig. 4c, in this setup gaseous CO_2 is delivered directly to the GDE through a flow field serpentine, where it reacts at the catalyst layer in close contact with an ion exchange membrane. This zero-gap architecture, differently from the flow cell configuration, eliminates the need for liquid catholyte, therefore only maintaining an electrolyte chamber within another flow field serpentine on the anode side. In this way, mass transport limitations and cell resistance are significantly reduced, and issues such as GDE flooding are mitigated due to the catalyst layer no longer being in direct contact with a bulk liquid electrolyte. As a result, MEAs can operate efficiently at industrially relevant current densities and offer strong potential for stacking and scale-up. Although the MEA system has been reported to significantly improve eCO_2RR performance [37,38], it still faces challenges in terms of stability and large overpotential, which differently from the current density has not improved when switching to this setup [17]. In fact, its long-term stability in industrial setting is still heavily hindered by the formation of precipitated salts, which happens due to the reaction of CO_2 with OH^- ions continuously generated at the cathode [39]. The precipitated salts accumulate on the electrode during operation, blocking the gas diffusion pathways in the electrode pores and consuming available CO_2 at the active sites by reacting with carbonate deposits and moisture to form bicarbonates, and accelerate cell failure [40]. While this configuration has allowed substantial improvement in selectivity towards CH_4, this is mainly due to the optimization of catalyst and membrane choice. Both anion (AEM) [41–43] and cation exchange membranes (CEM) [44] have been conventionally used with remarkable results.

Carbonate and bicarbonate-fed systems have also been developed more recently as an alternative to gas-fed systems. These systems enable CO_2 capture and conversion processes within a single step and eliminate the need for energy-intensive CO_2 desorption and purification steps. In this setup, CO_2 is released *in situ* at the electrode surface by protons generated from a bipolar membrane (BPM) that react with aqueous bicarbonate (HCO_3^-) or carbonate (CO_3^{2-}) solutions. This system offers effective carbon utilization that bypasses the energy-intensive step of extracting CO_2 from a CO_2 captured solution. However, the additional chemical equilibrium step of converting HCO_3^- to CO_2 can limit the availability of reactive species at the catalyst interface, potentially reducing the overall reaction rate. For CH_4 production, this poses a particular challenge, as methane formation requires high local CO_2 concentrations and efficient multi-electron transfer processes. While most bicarbonate-fed systems have demonstrated good performance for CO and formate, achieving high selectivity toward CH_4 remains difficult and typically requires highly active and stable catalysts [45]. More recently, Obasanjo et al. were able to operate a bicarbonate-fed system for 12 h at 500 mA/cm^2, maintaining FE for methane over 70 % [46].

5. Catalysts

5.1. Copper

The pioneering work of Hori et al. in the 1980s first demonstrated that CO_2 could be reduced to CH_4 at a copper electrode interface [47,48]. Since then, Cu as catalyst has been extensively studied, due to its properties that allow further reduction of CO_2 to hydrocarbon products, while other catalysts such as Ag, Au and Zn primarily yield CO with high selectivity. While this characteristic sets Cu apart from other catalysts explored so far, reduction to hydrocarbons still requires a high overpotential and suffers from poor selectivity due to the wide range of products that can be obtained [49] (shown in Fig. 5). Much effort has been devoted to understanding the process of reduction at Cu metallic interface, as well as tuning electrode structure and adjusting reaction process and conditions to achieve higher selectivity towards a specific product.

CO has been determined to be the crucial intermediate in eCO_2RR to methane, also backed up by DFT measurements [51–53]. First, *COOH is formed on the catalyst surface through a proton-coupled electron transfer step, which then produces *CO by dehydrogenation. The strength of *CO adsorption on the catalyst at this step plays a crucial role in determining the reaction pathway. *CO can either bind too strongly and block the active sites, suppressing CO production and favoring HER, or desorb from the catalyst, releasing CO as a main product. Only when *CO binding strength on a catalyst' surface is balanced (neither too strong nor too weak) can further reduction reactions proceed effectively,

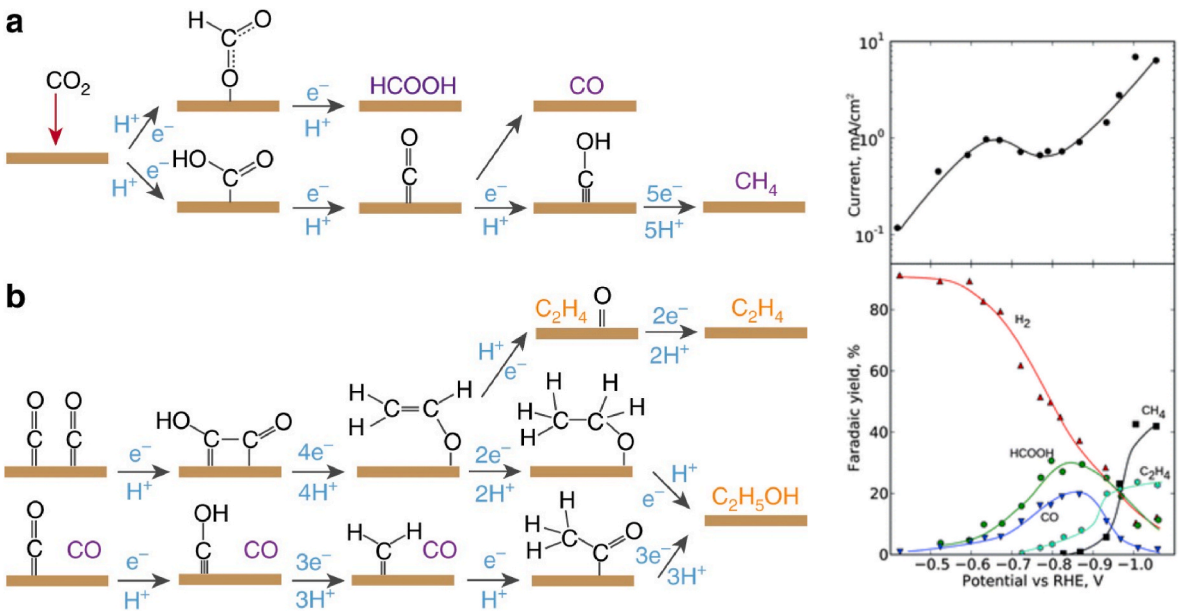

Fig. 5. Proposed mechanism for carbon dioxide electroreduction. (a) The pathway to C_1 products (formate, carbon monoxide, and methane) and (b) the pathway to C_2 products (ethylene and ethanol). Reproduced from [50], Copyright © 2018, The Author(s), licensed under CC BY. c) Products selectivity on Cu at different potentials, reproduced with permission from [51].

as established by Sabatier principle.

Schouten et al. observed two reaction pathways starting from CO: a C_1 pathway leading to CH_4 formation and a C_2 pathway leading mostly to ethylene formation [54]. These pathways differ in the key step of *CO protonation to *CHO, which ultimately leads towards methane (shown in Fig. 6), or *CO dimerization to *OCCO, initiating C-C coupling and leading towards ethylene and other C_2 products. The relative stability of either one of these intermediates dictates product selectivity. However, the main difficulty in optimizing one pathway is the presence of scaling relations, correlations between adsorption energies of key intermediates that make it difficult to independently optimize different reaction steps. This dependence manifests in practical tradeoffs: across a range of catalysts and applied potentials, the methane-ethylene relationship was found to be locked at nearly the same ratio, suggesting that the branching kinetics at the common intermediate are inherently constrained [55,56]. Breaking this dependence by selectively stabilizing one pathway over the other is therefore considered essential. Much effort has been devoted to tune selectivity towards either one by changing variables such as geometry, morphology, surface roughness or other chemical properties that affect chemisorption of reactive intermediates.

The stabilization of different intermediates is strongly potential-dependent [53]. Experimental and theoretical studies indicate that hydrocarbon formation occurs in the range of approximately −0.6 V to −0.9 V vs Reversible Hydrogen Electrode (RHE). At the lower end of this

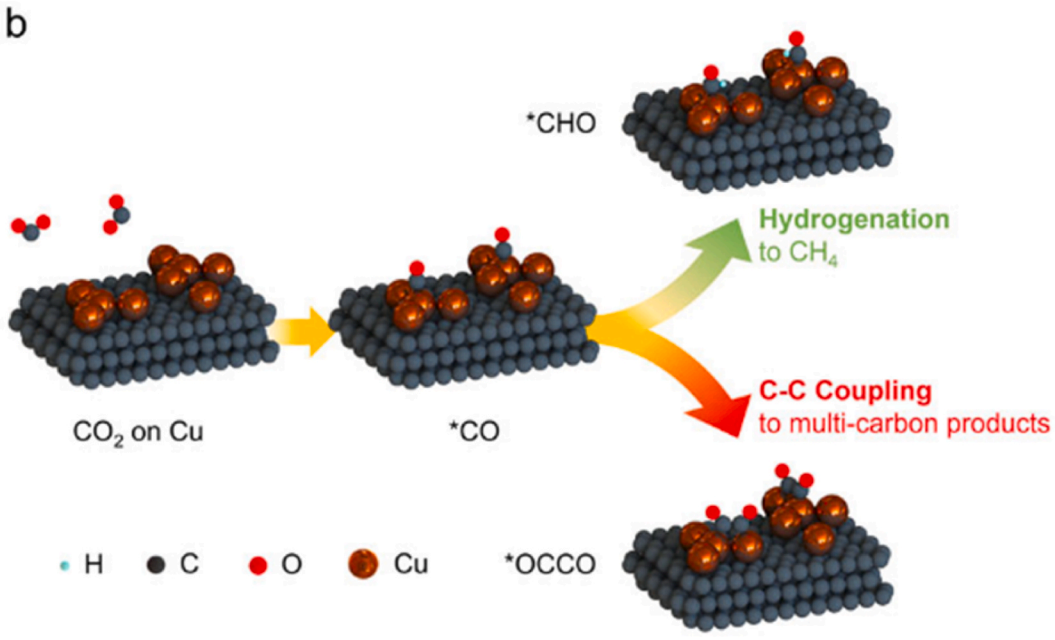

Fig. 6. Schematic of key reaction pathways for eCO_2RR: hydrogenation to *CHO for CH_4 production and C–C coupling to *OCCO leading to C_2 generation. Reproduced from [43], © 2021, The Author(s), licensed under CC BY.

window (around −0.6 V, where the barrier for CO dimerization is about 0.69 eV), ethylene formation is favored due to high CO coverage and strong CO binding, which promote C–C coupling. When much more negative or more positive potentials are applied, adsorbed hydrogen (*H) binds more strongly than CO, progressively displacing it from the active sites. This reduces surface CO coverage and suppresses the ethylene pathway. Within this potential window, the *CHO intermediate is often described as a common branching point, capable of leading either to methane (via sequential hydrogenation) or to ethylene (via C–C coupling) [57,58].

Later studies from Hori et al. explored various Cu-based catalysts (polycrystalline and single crystal) and determined the effect of surface orientation on product selectivity [59,60]: the C_1 pathway to methane production is mostly enhanced on single-crystal Cu(111) electrodes, while ethylene production is favored on Cu(100) electrodes. This facet dependence can be rationalized by the stabilization of different protonated CO intermediates due to a different geometric disposition (shown in Fig. 7). In fact, Cu(111) facilitates the formation of an alternative *COH intermediate, which makes the hydrogenation pathway more accessible and thus promotes CH_4 formation [61]. On Cu(100) instead, *CHO is more accessible and can either participate in C–C coupling with neighbouring CO*, form ethylene and other C_2 intermediates or hydrogenate stepwise to form methane, depending on the relative surface coverages of CO*, which are dictated by the applied potential [62–64]. The selective stabilization of *CHO versus *COH therefore accounts for the distinct behavior of Cu facets: *COH on Cu (111) biases selectivity toward C_1 products, while *CHO on Cu(100) enables both C_1 and C_2 pathways depending on applied potential which determines CO surface coverage.

Other works also reported that key intermediates such as *CO and *CHO were stabilized on stepped and kinked surfaces. This effect arises because atoms at step edges or kink sites have a lower coordination number (fewer nearest neighbors) compared to terrace atoms, which makes them more reactive and capable of binding *CO more strongly [66]. Scholten et al. reported that clean, flat, and atomically ordered surfaces favor hydrogen production, while defective and higher index surfaces lead to the generation of hydrocarbons, with higher yield of C_2/C_1 products on surfaces exhibiting a higher CO binding strength [51,65,67–69]. Durand et al. demonstrated that Cu(211) was the most active surface for CH_4 production, as it greatly stabilizes adsorbates and lowers reaction limiting potential with respect to (111) and (100); moreover, it tends to stabilize more CHO adsorption over CO adsorption, resulting in a much lower potential requirement for this specific pathway [65]. High-index crystal facets instead, such as Cu(311), Cu(511) and Cu (711), which show wider terraces with (100)-like geometry separated by steps, tend to be more active toward production of C_2H_4 and other C_2 and C_3 compounds, as they provide both the strong *CO binding of steps and the C–C coupling propensity of (100) terraces [63,65].

Several other strategies have been employed to finely tune the electronic structure of Cu, and in turn also the product selectivity. Incorporating foreign metal elements into the Cu lattice can either alter the electronic structure (via d-band center shifts, charge redistribution, and modified *CO/*H binding energies) or the geometric structure (ensemble size, strain, and interfacial effects), so as to affect adsorption energy and disposition of specific intermediates, effectively changing catalyst' activity and selectivity. Alloying Cu with metals like Ag [70,71], Fe [72], Au [73], or Zn [22,73] can improve methane selectivity by enhancing *CO binding and protonation [74], as the insertion of foreign elements moves the electronic bands away from Fermi level, resulting in an optimized binding energy for intermediates. Beyond alloying strategies, tandem catalysts have gained interest, due to their potential to aid multi-step reactions. In these systems, a CO-producing component

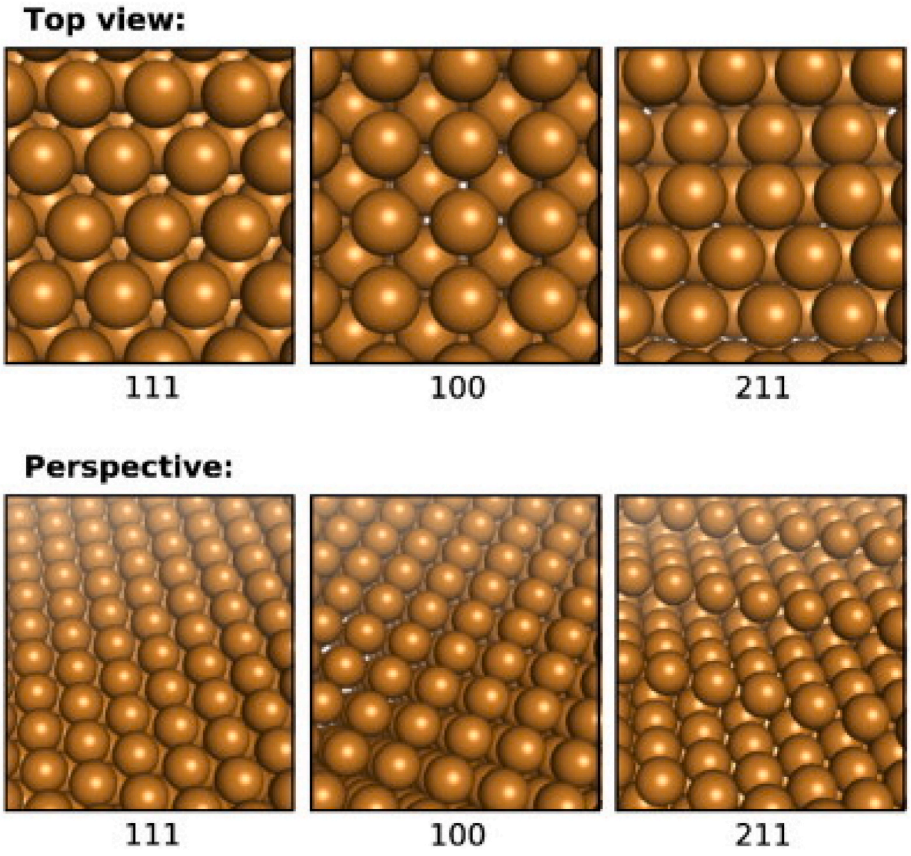

Fig. 7. The (111), (100), and (211) facets of the copper fcc crystal, as viewed directly and from perspective. 211 contains a terrace of atoms in the (111) geometry (with 3-fold coordination) and a step containing 4-fold coordination. Reproduced from [65] with permission.

such as Ag first converts CO_2 to CO, which then diffuses to adjacent Cu sites where hydrogenation proceeds toward CH_4. In this way, FE towards methane is increased due to a higher coverage of *CO on the modified Cu surface than bare Cu catalyst [70,75].

Despite the promising advantage of alloys, nanostructuring of Cu/Cu-based alloys remains essential for reaching high methane selectivity. As stated previously, the catalytic performance is strongly influenced by surface morphology, defect density, grain boundaries, and facet orientation. By engineering these features at the nanoscale, nanocatalysts can significantly enhance selectivity, as they can directly modulate adsorption energies, stabilize key reaction intermediates, and lower energy barriers along the methane formation pathway.

5.1.1. Nanostructures

With the advance in nanoparticle (NP) synthesis that allows to finely tune their dimension, composition, structure and morphology, nanostructured Cu catalysts in different shapes and sizes were explored in literature in order to tune surface chemisorption and resulting selectivity [76,77]. NPs present a clear advantage as catalyst in eCO_2RR with respect to their bulk counterpart due to their increased number of active sites as well as atoms on the corners, along the edges and in the crystal planes with different coordination numbers and chemical interaction energy. Smaller nanoparticles generally should enhance overall catalytic activity due to their higher surface-to-volume ratio and the presence of more high-energy reactive sites, such as edges and corners. However, understanding the size dependence of catalytic reactions remains complex, especially when multiple competing pathways coexist. Moreover, since different crystallographic facets can be stabilized on NPs with different shapes, different results are to be expected on different shapes [78] (as shown in Fig. 8).

For example, nanocubes (shown in Fig. 8b) are found to be more selective for ethylene, mostly due to their exposition of (100) surfaces and edge site atoms [81–84]. In fact, as (100) surfaces do not exclude pathway to methane, edge sites have been recognized as the main contributor to the shift in selectivity. This has been demonstrated by studies comparing nanocubes of different sizes: as the cube size increases, the proportion of corner and edge atoms decreases moving towards a surface configuration closer to one single crystal dominated by (100) planes. Loiudice et al. found optimal selectivity for ethylene in nanocubes with 44 nm edge length, suggesting that this result derives from an optimal balance between these plane- and edge-sites [81].

Contrasting results were instead found when analysing spherical NPs (depicted in Fig. 8a). Some studies report higher methane selectivity for smaller diameters [85,86], while others found HER to drastically surpass the activity for the eCO_2RR with sizes smaller than 20 nm [73,84]. Indeed, smaller diameters were linked to higher CO and H_2 formation, while bigger sizes were more selective towards hydrocarbons.

Studies involving copper nanoclusters (NCs) instead showed highest selectivity for methane in the particles with lowest size (0.5 nm) [27,87]. Recent studies and DFT calculations relate this increase in selectivity for smaller NPs to a lower coordination number, which favours the key step of *CO hydrogenation [43,44,88]. Another study on nano-octahedra NPs (Fig. 8c) investigated effects on selectivity of particles sizes in the range of 75–310 nm and found that the smallest dimension showed the best selectivity for methane [61,77]. This result was attributed to geometrical effect, given by the high presence of corners and edge exposing (110) and (100) planes.

A phenomenon similar to the particle size effect was also observed in nanowires (NWs) (Fig. 8d): depending on the length and density, the local pH is modulated, influencing either pathway over the other. Ma et al. found that as the Cu NW arrays grew longer and denser, the FE for H_2 production steadily decreased as the amount of CO_2 reduction products increased, and, particularly, the FE for C_2H_4 gradually increased with increasing the length of Cu NWs [89]. However, no C_1

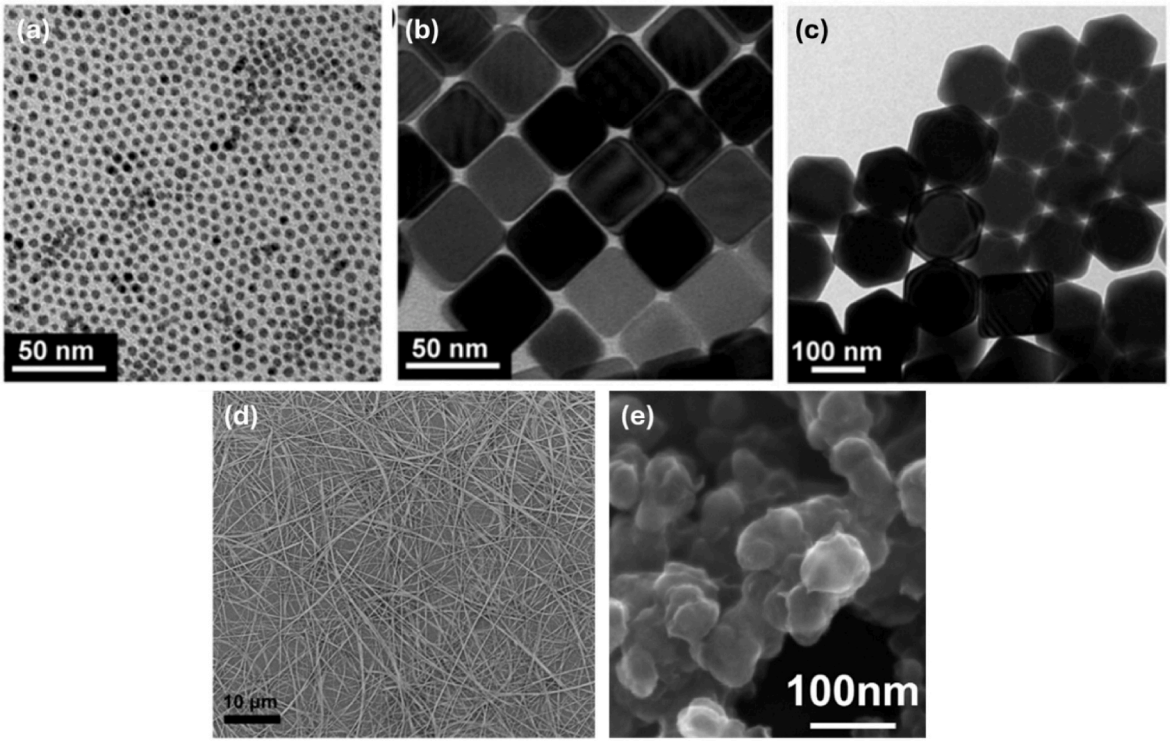

Fig. 8. SEM images of different nanostructured Cu based catalyst used in eCO_2RR: (a) spherical, (b) cubical NPs, where dominant (100) facets favor C-C coupling to ethylene (c) octahedral NPs, which are enriched with (100) facets and promote C_1 products, adapted with permission from [61], Copyright © 2020 American Chemical Society; (d) Cu nanowires, which depending on length can offer edge sites and steer selectivity towards C_2 or C_1 products, reproduced with permission from [79], Copyright © 2017 American Chemical Society; (e) a molecular copper-porphyrin complex, which provides well-defined coordination environments that mimic enzymatic active sites and stabilize key intermediates along methane pathway, adapted with permission from [80], Copyright © 2016, American Chemical Society.

products were observed. Li et al. instead investigated a 20 nm-diameter 5-fold twinned ultra thin Cu nanowire which exhibited a FE for CH_4 of 55 % due to the high presence of low coordination edge sites [79]. However, this effect may be mostly due to the insertion of twin boundaries, which have been reported to significantly lower interfacial energy, while enhancing mechanical strength, electrical conductivity, thermal stability and methane selectivity [21]. For instance, a copper twin-boundary reported an intrinsic faradaic efficiency for methane of 92 % at a current density >1 A/cm^2.

Cu single atom catalysts (SACs) have also received attention recently, as their isolated active sites should reduce C-C coupling and potentially result in a higher selectivity towards CH_4 [90–92]. In fact, a few have been reported to improve selectivity, while also allowing to reach industrial compelling current densities (>100 mA/cm^2), especially when paired with supporting carbon (such as graphene) or porous molecular structures for enhanced stability and improved electrical conductivity [31,44,93–95]. Alongside SACs, other metal complexes and molecular structures have been explored, because they possess well-defined atomic structures whose electronic states can be tuned. Particularly, metal–organic frameworks (MOFs), known for their high porosity and specific surface area, have emerged as a promising platform for spatially isolating metal atoms in an atomically dispersed state. More importantly, the inherent structural and compositional tunability of MOFs allows precise control over the coordination environment of single-atom catalysts, enabling customized catalytic properties. Among various MOFs, porphyrin-based ones (reported in Fig. 8e) have gained attention due to their nitrogen-rich structures, which readily coordinate with a range of transition metal ions via the central nitrogen sites, facilitating the formation of transition metal-based SACs [80,96–99].

Among molecular structures, of particular interest are nitrogen-doped carbon frameworks with Cu−N_x configurations [100], where copper atoms are coordinated with nitrogen within a carbon matrix, mimicking enzymatic centers, and are known to promote catalytic reactions with high selectivity and stability. Similarly, copper phthalocyanine (CuPc), a macrocyclic complex featuring a Cu–N_4 core, has demonstrated outstanding catalytic performance due to its ability to be reversibly restructured to Cu nanoclusters, which aid CH_4 formation [23]. These materials seem to be highly promising, as they bridge the gap between heterogeneous and homogeneous catalysis, exploiting the well-defined active centers of molecular catalysts while also offering the durability and recyclability of solid-state systems.

5.1.2. Cu reconstruction and oxidation states

While all these nanostructures report high catalytic activity, their main limitation lies in the process of surface reconstruction, the tendency for nanoscale metal-based catalysts to change in morphology, shape, size or oxidation state during eCO_2RR, causing activity degradation or even a shift in selectivity. The reconstruction of electrocatalysts typically involves the dissolution of metal ions when the catalyst comes into contact with the electrolyte and interacts with reaction intermediates. These dissolved metal ions can then redeposit under a reductive potential. However, the specific reconstruction mechanism changes depending on initial catalyst structure and morphology. For instance, polycrystalline Cu has been found to reconstruct to Cu(100), probably due to CO* poisoning [101]. Other studies report that Cu NPs tend to aggregate to create disordered structures, changing disposition of active sites and therefore causing product selectivity to have a shift towards ethylene [102].

The reconstruction of the Cu surface by oxidation has also been found to have a great impact on the activity and product selectivity [103]. In fact, copper exhibits multiple stable oxidation states (Cu^0, Cu^+, and Cu^{2+}), each with distinct electronic properties that influence the adsorption and stabilization of key reaction intermediates, tuning performance either toward methane or ethylene and other C_{2+} compounds. Particularly, the presence of Cu^+ sites has been widely associated with enhanced selectivity toward C–C coupling products like ethylene [104], due to its ability to stabilize the *OCCOH intermediate with respect to the Cu^0 counterpart.

More recently, Cu^{2+} has also drawn attention, despite being generally considered unstable as it tends to reduce to Cu^+ or Cu^0 during operation. As more oxidized states increase progressively *CO adsorption energy, Cu^{2+} sites are reported to favor sequential hydrogenation of *CO to *CHO/*COH and ultimately CH_4 rather than *CO dimerization due to the stronger electrostatic interaction [32]. However, under the reductive potentials applied during operation, Cu^{2+} is not thermodynamically stable and inevitably transforms into lower-valent copper species (Cu^+ or Cu^0), contributing to the formation of oxide-derived copper (OD-Cu) catalysts, which often exhibit mixed-valence states with interfacial regions of Cu^+ and Cu^0. These interfaces are reported to be more selective for C_{2+} product formation: in fact, surfaces exhibiting a balanced mixture of Cu^+/Cu^0 achieved significantly higher FEs for C_{2+} products, while surfaces dominated by Cu^0 mostly favored CH_4 production [105,106]. The stabilization of Cu^{2+} ions therefore remains complex, although some strategies are being developed: for instance, optimizing structural coordination [107], embedding the ions into robust oxide lattices, MOFs [108,109] or solid solutions can stabilize the valence state, prevent complete reduction by hindering electron transfer. Zhou et al. were able to stabilize Cu^{2+} by incorporating them into a protective CeO_2 matrix, reaching a FE of 67.8 % for CH_4 [32] (depicted in Fig. 9). While tuning the oxidation state of copper seems to deliver promising results, future research is still needed in order to achieve reliable and stable control over Cu oxidation states.

Overall, as methane production in CO_2RR is intimately linked to the catalyst's atomic structure, surface facets, defect density, and electronic properties, its selectivity is strongly favored by catalyst designs that stabilize the *COH intermediate and promote sequential hydrogenation, as exemplified by Cu(111), stepped facets such as Cu(211), and low-coordination sites in nanostructures. Strategies such as facet engineering, defect introduction, alloying, nanostructuring (particularly through manipulation of particle size, shape, composition) and the development of single-atom and molecular Cu catalysts have shown significant promise in tuning the adsorption energies of key intermediates to overcome the inherent scaling relations that otherwise lock product distributions. Exploiting specific oxidation states of copper emerges as another promising direction to increase selectivity. Yet, despite their high activity, these advanced structures often suffer from surface reconstruction or valence change under operating conditions, leading to a shift in product selectivity. Moving forward, great effort should be devoted to stabilize these structures and obtain consistent and scalable methane production. The integration of these design strategies with supporting frameworks and matrices offers a compelling path to achieve both high selectivity and long-term stability.

5.2. Other catalysts

While copper remains the benchmark catalyst for CO_2 reduction to most hydrocarbons including methane, its broad product distribution, modest selectivity, high overpotential and limited stability have motivated exploration of other materials. Other alternative catalysts are far less explored and consequently their experimental demonstrations remain scarce, although theoretical studies and DFT calculations indicate significant promise.

Early studies identified certain noble metals, such as Pt, Pd and Ru, as capable of catalyzing CO_2 reduction to methane under specific conditions [110], although not as the main product. Their high hydrogenation activity suggests potential for driving the stepwise reduction of adsorbed CO intermediates toward CH_4. However, in aqueous electrolytes, these metals mostly overwhelmingly favor the competing HER, producing methane only in trace amounts [111]. Their tendency toward strong proton reduction, combined with insufficient binding energy balance to stabilize CH_4 intermediates, has so far limited their viability compared to copper.

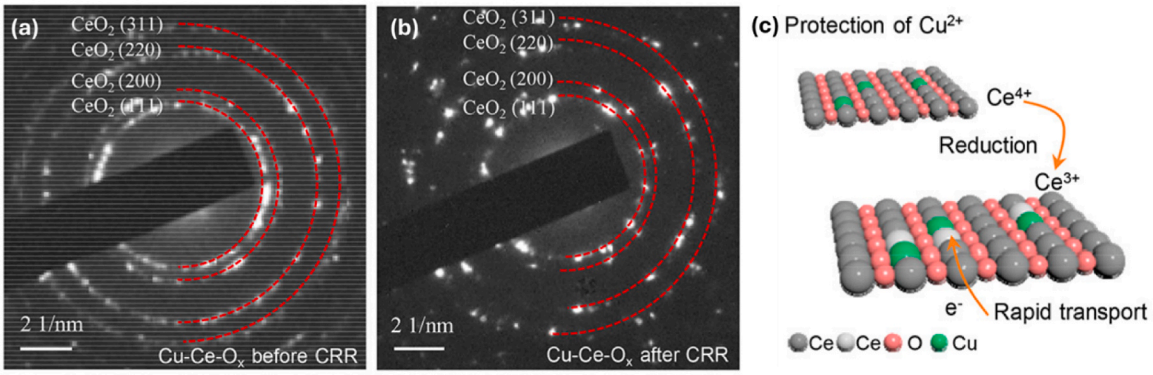

Fig. 9. Selected Area Electron Diffraction (SAED) patterns of Cu-Ce-O_x (a) before operation and (b) after operation; (c) scheme of the mechanism of the self-sacrificing Ce-O_x matrix to protect Cu^{2+} ions. Adapted with permission from [32], Copyright © 2022, American Chemical Society.

For instance, Pt was first discarded as catalyst for the eCO_2RR as it suffers from deactivation due to formation of CO_{ads} that heavily poisons the catalyst. However, it has been gaining attention recently with the development of MEAs, as this configuration allows more control on the CO_{ads} coverage and enables high faradaic efficiency towards methane. In particular, since reduction of CO_{ads} to methane is assisted by H_{UPD} (which represents hydrogen adsorbed on the Pt surface at potentials more positive than the equilibrium potential for HER), the reaction is able to proceed at potentials close to its thermodynamic equilibrium [112,113]. Additionally Pt is gaining interest due to its notable stability in both alkaline and acidic media, which could maintain long term operation provided that the catalyst is strategically designed to steer from HER to methane selectivity [114].

Building on insights from copper, similar catalyst design strategies have been applied to other metals to enhance CH_4 selectivity. For instance, as previously discussed, SACs have been determined to be very promising for methane formation. Recent theoretical and experimental studies suggest that, similar to Cu, other metals may also display strong dependence on their coordination environment and local geometry, possibly making copper-based design strategies transferable to optimize pathway to methane formation [115,116]. Moreover, first-principles studies are being conducted to explore and combine different materials with the goal of tuning their electronic structure and obtain a lower potential barrier. Few studies tested different transition metal single atoms supported on TiC and TiN, which due to their tailorable electronic features show a remarkably low reaction overpotential [117,118]. Two-dimensional materials such as graphene have also been investigated by DFT studies as support, due to their high surface area and highly tunable electronic structure [119,120]. DFT studies on N-doped graphene sheets doped with Fe, Co, or Ni have revealed distinct catalytic pathways, with Co-doped graphene achieving particularly low limiting potentials [121]. Single Zn atoms supported on defective graphene were predicted to favor CH_4 formation at lower overpotentials than Cu (−0.83 V vs. RHE) [122], and theoretical calculations show that Zn atoms should inhibit CO generation as it links to the O atom rather than the C, therefore blocking the generation of CO and helping to produce CH_4. Experimentally, Han et al. demonstrated methane production with Zn-based SACs on N-doped carbon, achieving 85 % faradaic efficiency, although at modest current densities [123]. This result provides direct evidence that copper-free elements can indeed catalyze methane formation.

In summary, while copper continues to dominate CO_2RR research, few studies are emerging on alternative catalysts to overcome the main downsides of Cu-based systems. Although the field is still in its early stages and shows limited experimental validation, theoretical predictions and initial experimental breakthroughs highlight that non-Cu catalysts hold strong promise for achieving lower overpotentials and new pathways for methane production. Nevertheless, deeper mechanistic understanding and extensive experimental efforts are still needed before these systems can progress significantly, and their industrial implementation remains a distant prospect.

6. Operative conditions

The great advantage of electrochemical reactions consists in being able to be carried out at standard conditions of both temperature and pressure. While the temperature is generally maintained between 20 and 30 °C, some studies explore elevated temperatures, up to around 60 °C, to assess effect on reaction kinetics and simulate industrial conditions. In fact, while pressure does not seem to impact significantly on the reaction seelctivity [124], temperature modulation has been found to deeply influence product selectivity. Koper's group has determined that methane selectivity decreases with increasing temperature up until 48 °C, while HER completely dominates at temperatures over this threshold [125]. This change in selectivity is attributed to an increase in local pH caused by higher rate of OH^- formation.

Hori et al. first suggested the pH environment to be a crucial parameter for determining the reaction selectivity [126]. Later studies confirmed this correlation [127–129], but mostly attributed this high influence to the local interfacial pH. An acidic local pH is beneficial for both HER and methane selectivity as it favours the defining step of CO protonation, responsible for shifting the selectivity towards methane and therefore inhibiting ethylene production. However, maintaining an acidic environment is not trivial as the reaction continually produces OH^- ions. In this case, the choice of electrolyte becomes a critical factor for suppressing local pH increase depending on its buffer capacity. It has been determined that high concentrations of bicarbonate cause the bulk pH to be closer to neutral, favouring methane formation [128].

Besides the (bi)carbonate concentration, different studies have also focused on the role of alkali metal cations in the electrolyte and how they are able to influence selectivity on Cu. It has been confirmed that selectivity for C_2 products grows following the trend $Cs^+ > Rb^+ > K^+ > Na^+ > Li^+$, while enhanced methane formation mostly follows the opposite trend [128,130–133]. Different explanations have been proposed for how cations cause this effect, relating it to variations in adsorption kinetics and local electric field strength. The Norskov group suggested that accumulation of alkali metal cations at the electrode–electrolyte interface modulates the electric field at the interface, modifying stabilization of reaction intermediates [130,134].

To enhance the solubility of CO_2 in aqueous systems, Kaneco et al. employed methanol in combination with various sodium-based supporting electrolytes. Their study reported relatively large methane efficiency for all of them (≥43.4 %) and a maximum methane efficiency of 70 % using a $NaClO_4$/methanol-based electrolyte [25]. Some studies also implement binders as strategy to control the local pH and increase efficiency towards methane [135,136].

As a strategy to regulate local CO_2 availability at the catalytic sites and promote the methane pathway over C–C coupling, Wang et al. investigated the impact of using a more diluted CO_2 feed [137]. In fact, they were able to achieve a methane FE of 48 % with a gas stream containing 75 % CO_2.

In conclusion, while elevated temperatures generally suppress CH_4 formation in favor of hydrogen, the decisive factor is represented by interfacial pH, with mildly acidic conditions favoring CO protonation over C-C coupling. Since maintaining this environment is challenging, electrolyte composition becomes critical: smaller cations (Na^+, Li^+) promote CH_4, while larger cations favor C_2 products. Overall, precise control of local pH and electrolyte chemistry remains the most effective strategy for steering the reaction toward methane. Adjusting feed composition represents another promising direction, but further studies are required to evaluate how CO_2 availability and the presence of different co-feeds or gas mixtures influence the reaction pathway and methane selectivity.

7. Scale up

While extensive progress has been made in the laboratory on catalyst engineering and understanding reaction mechanisms, the transition to commercial-scale CH_4 production presents significant technical and economic challenges. Obtaining methane as major product is still challenging at increasing current densities and the electrochemical conversion of CO_2-to-CH_4 lacks sufficient stability, carbon utilization, and energy efficiency [138].

At commercial scales, conventional H-cell systems are impractical due to mass transport limitations. The popularization of gas-diffusion electrodes, which enhance CO_2 availability, product removal and overall water control in the cell, has made flow cells and MEAs the most promising configurations for industrial-scale operation. Key engineering goals include maintaining current densities larger than 200 mA/cm^2, minimizing cell voltages (<3 V), and managing gas-liquid interfaces to avoid flooding and carbonate formation in order to considerably improve stability. Industrial implementation also requires a robust supply of CO_2 from flue gas, direct air capture, or other biogenic sources, although impurities present in these streams can often degrade catalysts and membranes. Therefore, the electrolysis system must be compatible with variable CO_2 purity or include pre-treatment processes.

Finally, to be economically and environmentally viable, CO_2-to-CH_4 systems should be able to integrate with intermittent renewable energy sources and still achieve total energy efficiencies exceeding 30 %. This includes not only electrochemical performance but also downstream gas separation, compression, and system thermal management. Lifecycle assessments must demonstrate a net reduction in CO_2 emissions compared to conventional methane synthesis methods (e.g., the Sabatier process).

Currently, very few projects focusing on scaling up this technology are being developed. Opus Twelve, funded by SoCalGas and PG&E, has investigated a method to convert CO_2 in raw biogas to methane in a single electrochemical step, employing a stack of PEM electrolyzers [139]. Another potentially promising project consists in an initial scale up to 81 cm^2 of active area in MEA, performed by Xu et al. [140]. They employed di-amino-triazole (DAT) as catalyst and were able to reach a FE_{CH4} of 54 % at a total current of 10 A (123 mA/cm^2). Other promising results found in literature, that were able to obtain a FE_{CH4} higher than 50 % at technoeconomic compelling current densities (>100 mA/cm^2) are reported in Table 1. However, it has to be highlighted that all these collected results refer to small scale (i.e. few cm^2) electrodes, once again confirming the technical challenges associated with this process. This demonstrates that the path has been laid out, but research still needs to be pushed forward toward the preparation of large-scale electrodes for methane production, similar to what is happening with other eCO_2RR products [141].

7.1. Interdependencies and trade-offs in key performance indicators

As analyzed in the previous sections, the electrochemical reduction of CO_2 to methane is a complex process influenced by multiple, often interdependent, performance indicators. Understanding the correlations and trade-offs between these variables is essential, as improvements in one metric frequently come at the expense of another, especially when dealing with scaling up of the system.

Previous studies have consistently reported trade-offs among key performance indicators in CO_2RR. One widely observed relationship is the trade-off between current density and applied potential: operating at higher, industrially relevant current densities typically requires a larger

Table 1
Comparison of relevant results employing different catalysts and setup from literature obtained at technoeconomic compelling current densities. TDPP: diamino-triazine; CuTAPP: donor–acceptor modified Cu porphyrin; SAS: single atom site; Fc-CPP-Cu: Cu-porphyrin based conjugated porous polymers, Fc: ferrocenyl. DBC: dibenzo-[g,p]chrysene-2,3,6,7,10,11,14,15-octaol, 8OH-DBC.

Catalyst	Electrolyte	Reactor	Current density (mA cm^{-2})	Electrode size (cm^2)	Membrane	FE_{CH4}	Ref.
200 nm sputtered Cu	1.5 M $KHCO_3$	flow cell	250	–	AEM	48 %	28
Cu single-atoms/hydrogenated Graphene	1.0 M KOH	MEA	200	0.5	AEM	70 %	90
Cu-TDPP	0.5 M PBS	flow cell	183	0.5	AEM	71 %	96
Fe phthalocyanine/Cu	1.0 M $KHCO_3$	flow cell	128	1	AEM	64 %	31
Cu-Ce-Ox	1 M KOH	flow cell	200	–	AEM	68 %	32
Ga doped CuAl	1.0 M $KHCO_3$	flow cell	109	–	AEM	53 %	29
Au-Cu	1 M $KHCO_3$	flow cell	112	1	AEM	56 %	33
0.5 nm Cu NCs	1 M KOH +2 M KCl	flow cell	1500	–	AEM	80 %	27
La_2CuO_4	1 M KOH	flow cell	205	3	AEM	56.3 %	142
Cu phthalocyanine	0.005 M H_2SO_4	MEA	100	–	BPM	71 %	135
CNP/Cu phthalocyanine	0.05 M $KHCO_3$	MEA	136	5	AEM	62 %	43
Cu NPs over N-doped carbon	0.1 M $KHCO_3$	MEA	320	4	AEM	73.40 %	42
Cu mesh	0.3 M $KHCO_3$	MEA	500	2	AEM, BPM	75 %	46
B-doped Cu–N	1 M KOH	MEA	300	0.6	PEM	73 %	44
La_5Cu_{95}	1 M KOH	MEA	193.5	4	AEM	64.50 %	143
°3,5-diamino-1,2,4-triazole	0.1 M $KHCO_3$	MEA	123	4	AEM	50 %	140
18-Crown-6/CuNPs	$H2SO_4$ + $K2SO_4$	flow cell	600	–	PEM	51 %	144
CuTAPP	1 M KOH	flow cell	290	1	AEM	54 %	97
Cu SAS in MOF	1 M KOH	flow cell	420	–	AEM	81 %	145
Fc-CPP-Cu	1 M KOH	flow cell	200	0.5	AEM	>70 %	98
Poly-Cu	1M KOH	flow cell	192	1	AEM	64 %	146
Cu-DBC	1M KOH	flow cell	203	0.25	AEM	80 %	108
Ir_1–Cu_3N/Cu_2O	1M KOH	flow cell	320	1	AEM	75 %	147

overpotential, as illustrated by polarization curves (current–voltage behavior) reported in multiple studies [148,149]. This increase in potential directly impacts energy efficiency by raising the overall power consumption of the system and therefore production cost, presenting a key challenge for scaling up.

Another important trade-off involves FE and current density. Several works have shown that increasing current density often leads to a decrease in FE, due to enhanced competition from side reactions such as hydrogen production and limitations in CO_2 mass transport to the catalyst surface. This translates in another competition between FE and single pass conversion (SPC): low CO_2 feed flow rates can enhance SPC by allowing more complete CO_2 utilization within a single pass, but this frequently comes at the cost of reduced FE [150,151]. This reduction stems from local depletion of CO_2 at reactive sites, which not only lowers FE but also limits the maximum current density achievable under such conditions.

Additionally, a trade-off arises between stability and current density [152], as a higher current density generally accelerate catalyst degradation and reduce FE. Consequently, achieving high production rates often comes at the expense of durability, as systems operated at elevated current densities exhibit more rapid performance decay and lower FE over extended timescales.

Among these key performance indicators, cell potential, faradaic efficiency, current density, and operational stability are then central to evaluating catalyst and cell performance. To qualitatively test whether these widely assumed relationships emerge systematically from reported data, a brief multi-variate analysis was conducted on a small dataset of experiments found in literature. The dataset was constructed by integrating results from Table 1 with others reported in literature [17]. Operating potential was converted to cell voltage by assuming a combined anodic, membrane, and electrolyte overpotential contribution of 1.5 V [153] in order to have uniform samples.

First, a Principal Component Analysis (PCA) was performed on the selected dataset. PCA is an unsupervised multivariate technique that reduces the dimensionality of a dataset by projecting it onto new orthogonal axes (principal components) [154]. Each component is a linear combination of the original variables and is ordered according to the amount of variance it explains in the data. This allows one to visualize how these performance indicators vary together, uncover correlations between them, and detect outliers.

The PCA revealed that a small number of principal components (PC1 and PC2) captured most of the variance in the dataset. Scores plots of PC1 vs. PC2 were used to illustrate the distribution of samples along the main axes of variance, allowing for the identification of groups of experiments and potential outliers. Loading plots were included in parallel to show the contribution of each performance indicator to the principal components, providing insights into how individual variables contribute to the main axes of variability in the dataset. Variables with large loadings of the same sign on a given component are positively correlated along that mode of variability, whereas variables with large loadings of opposite signs are negatively correlated. Conversely, variables with small loadings contribute little to that component and exhibit weak correlation in that direction.

In the present analysis FE and voltage displayed strong negative loadings on PC1 (see Fig. 10a), indicating that these variables usually vary together along the dominant trend in the data. Current density also exhibited a negative loading on PC1, but with a smaller magnitude, suggesting a weaker positive correlation with both FE and voltage in this variability mode. While these relationships are specific to each principal component, they can be interpreted as patterns of shared variance between these performance descriptors. This relationship is visible in different articles from the dataset, where experiments performed at high current density and showing high FE also show higher potential [42,43,135]. The fact that this trend emerges cleanly in PCA confirms its robustness across different reports and catalyst designs.

On PC2 (Fig. 10b), FE and current density contributed with negative loadings, while stability and cell voltage displayed strong positive loadings. Thus, PC2 captures a secondary trade-off in the dataset: experiments characterized by higher FE and current density are generally associated with lower stability and reduced cell voltage, whereas stable operation is correlated with higher cell voltage but lower selectivity and productivity. This correlation emerges again in numerous samples from the dataset [27,44,46,144]. Again, this is consistent with prior qualitative discussions in the field, but here it is quantitatively confirmed across multiple independent studies employing different catalysts.

In the sample plot (Fig. 10c), along PC1 (y axis), samples were distributed across both positive and negative scores, indicating that the dataset contains distinct regimes of performance. The balanced spread of samples across this axis suggests that multiple performance regimes are represented in the dataset rather than a single dominant trend. Looking at PC2 samples instead, the majority of sample scores were located near the origin of PC2 (x axis), indicating that while the productivity-stability trade-off is present, it is statistically less dominant than the FE-voltage-current relationship.

To complement the analysis, a Partial Least Squares (PLS) regression model was also calculated and applied to the same dataset. PLS is a supervised regression technique designed to model the relationships between a set of predictor variables (X) and one or more response variables (Y) [155]. Unlike PCA, which only considers the variance within the predictors, PLS extracts latent variables (LVs) that maximize the covariance between X and Y. In this analysis, methane selectivity was chosen as a response, aiming to identify which of the others experimental parameters are most strongly associated with this specific performance outcome.

Latent Variable 1 (LV1), whose loadings are shown in Fig. 11a, explained a substantial portion of the covariance between predictors and

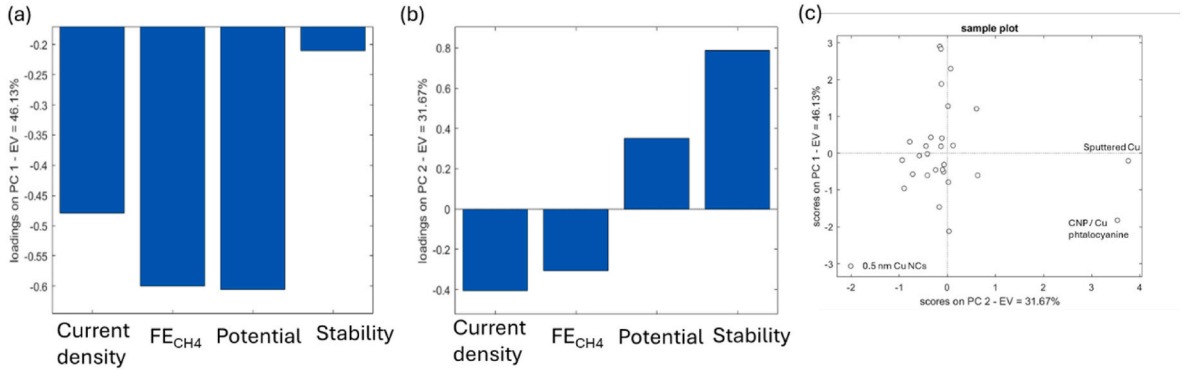

Fig. 10. Variable loadings of (a) PC1 and (b) PC2. Loadings define how much each single variable affects distribution on the PC; (c) Sample scores on the plane defined by PC1 (y axis) and PC2 (x axis). The position of sample points along x axis is governed by variable loading of PC2 and along y axis by loadings of PC1.

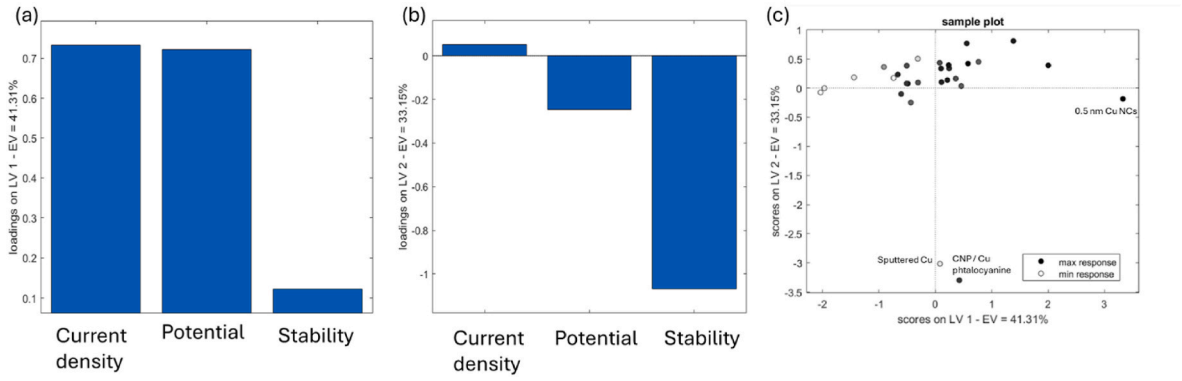

Fig. 11. Variable loadings of (a) LV1 and (b) LV2. Loadings define how much each single variable affects the response (Faradaic efficiency); (c) sample plot of LV2 vs LV1. As for the PCA, position of sample points along x axis is governed by variable loading of LV1 and along y axis by loadings of LV2.

response. In this component, potential and current density exhibited similar loadings, confirming the general trend that higher currents are typically linked to higher cell potentials. This axis also aligned positively with FE, indicating that improved selectivity is commonly achieved at the cost of higher energetic input. These contributions govern the x-axis of the sample plot (Fig. 11c), showing a mostly uniform distribution of samples; however, samples that present a higher response (higher FE) are mostly located in the positive quadrant, suggesting current density and potential to be more impactful in the current dataset. Again, the trade-off between higher FE and higher potential at industrially relevant current density is suggested. LV2 (Fig. 11b) instead, which represents the y-axis on the sample plot, shows a much higher stability contribution, while current density and potential are much less present. While most of the samples seem to not be affected by stability, it is possible to find some outliers, which are highlighted in the score plot.

Overall, PCA revealed that the dataset is structured around a small number of dominant trade-offs: on PC1, faradaic efficiency, cell potential and current density opposed stability, while PC2 contrasted selectivity/productivity with stability and cell voltage. PLS analysis complemented these findings by directly relating operational parameters to methane selectivity, showing that the main correlation (LV1) links higher current densities with potentials, while an alternative regime (LV2) showed an opposite correlation between stability and FE, highlighting difficulty of maintaining high selectivity for long term measurements.

The present analysis serves primarily as a qualitative confirmation of established interdependencies between key performance indicators this field. However, both analyses identified three main outliers that deviate from the general patterns found in the dataset. The first corresponds to the work of Gabardo et al. [156], which utilized sputtered copper as catalyst, resulting in very high operational stability (100 h) but low selectivity toward methane as the system targeted C_2 products. A second outlier, reported by Xu et al., who employed carbon nanoparticles combined with copper phthalocyanine, achieving relatively high faradaic efficiency together with exceptional stability exceeding 100 h [43]. Finally, the last outlier corresponds to the work of Salehi et al., which investigated copper nanoclusters as a catalyst, obtaining very high faradaic efficiency and current density compared to the majority of reported systems [27]. Specifically, these last two samples illustrate how specific catalyst designs can circumvent the general trade-offs and trends observed in the broader dataset. Indeed, such cases represent promising strategies for overcoming the otherwise consistent trade-offs observed across the literature and therefore warrant further investigation as promising directions for advancing eCO_2RR performance towards methane.

8. Technoeconomic analysis

A thorough and comprehensive TEA of an electrochemical system for methane production is essential to evaluate the viability of this emerging technology from multiple perspectives. Such an analysis not only provides critical insights into the economic feasibility and cost structure of the process, but also serves as a key metric for assessing its environmental sustainability and potential competitiveness with respect to more established and commercially deployed methane synthesis methods. In particular, understanding the capital and operational expenditures, energy demands, conversion efficiencies, and scalability of electrochemical methane production routes is fundamental to determine their suitability for integration into energy systems oriented toward decarbonization and circular carbon management.

Despite growing interest in eCO_2RR, the techno-economic landscape of processes specifically targeting methane remains largely underexplored. Numerous TEAs have been carried out in recent years focusing on eCO_2RR technologies, but methane is only occasionally included among the potential products evaluated [157–159]. In fact, these studies often center on broader product distributions or emphasize other reduction targets such as carbon monoxide, formate, ethylene, or alcohols, leaving methane electrosynthesis insufficiently investigated from a dedicated process engineering standpoint. To the best of our knowledge, only a limited number of works have directly addressed the economic and technical aspects of methane production via electrochemical routes, assuming CO_2 feedstocks derived from point sources such as industrial flue gases, or even more dilute streams like ambient air and seawater [160,161]. Based on the few data present in the literature, we collected different key economic metrics and operational parameters employed in the TEAs, which are reported in Table 2.

The table clearly shows that, despite the selection of ambitious performance parameters in terms of currents and selectivity, the calculated cost of methane production remains, in most cases, far above the current market price, which is less than 0.2 $/kg [162]. This high cost is mainly attributed to the current high cost of electricity, which dominates (in the range 40–60 %) all other items of expenditure [159]. Moreover, also the costs associated with the CO_2 capture heavily contribute to the technology OPEX, especially for gas mixtures containing low (<20 %) concentrations of CO_2. In any case, it is worth noticing that this production cost is in line with other analyses provided in the literature for eCO_2RR and other general power-to-methane systems [11,163,164].

Going into details on studies focused only on methane production, Wu et al. [160] investigated the economic aspects of CO_2 electroreduction to CH_4 using CO_2 sourced from industrial flue gases. Their analysis incorporated several key cost components: CO_2 capture at a price range of $30–60 per ton; capital investment for a capture facility capable of processing 100,000 tons annually estimated at $27 million;

Table 2
Comparison of relevant economic metrics and operational parameters employed in the TEAs of CO_2 electroreduction to CH_4. CAPEX: Capital Expenditure; OPEX: Operating Expenditure; y: year; —: data not provided. Regarding cell potential values, positive values are referred to voltage (V), while negative ones are referred to potential (V vs RHE).

Metric/Parameter	Ref. [158]	Ref. [160]	Ref. [161]	Ref. [159]
FE_{CH4} (%)	90	90	85	50
Current density (A/cm^2)	–	–	0.5	1
Voltage (V)/Potential (V vs RHE)	–	−1.30	4.00	−1.06
Carbon utilization (%)	–	60	–	–
Energy conversion efficiency (%)	60	–	–	–
CH_4 productivity (ton/y)	–	34333	29565	101
Lifetime (y)	–	–	7	20
Working hours (h/y)	–	8000	–	–
Electricity cost ($/kWh)	0.020	0.091	0.049	0.061
CO_2 capture cost ($/ton)	30	30	277	–
Total CAPEX (M$)	–	59.7	313.7	–
Total OPEX (M$/y)	–	71.3	133.3	–
Electrolyzer cost ($/kW)	500	300	221	–
CH_4 production cost ($/Kg)	0.8	0.3	5.4	5.7

electrolysis parameters assuming 90 % FE for methane and 10 % for hydrogen at a potential of −1.3 V vs RHE; an electricity cost of 0.091 $/kWh resulting in an annual energy expenditure of $4.5 million; and a projected cost of $20 million for the electrolyzer stack based on a price of 300 $/kW. The electrolyzer was assumed to operate for 8000 h per year, with maintenance costs around 2.5 %. Gas separation, crucial to the process, was carried out through Pressure Swing Adsorption (PSA, see section 9.1), selected for its relative efficiency. Their findings revealed that even under optimized operating conditions, the combination of high electrical energy consumption (high electrovalency) and the low market value of methane render the process economically unfeasible at present. However, the authors emphasized the potential of this technology in future applications, particularly as a sustainable energy storage medium or even as a method for *in situ* fuel production in extraterrestrial environments—such as producing methane-based rocket fuel on Mars, a concept relevant to human space exploration. Interestingly, they also noted that selectivity toward methane had a lesser impact on profitability than anticipated, primarily because hydrogen—the major byproduct—is significantly more valuable, at approximately 5.09 $/kg.

Similarly, Welch et al. [161] analyzed the cost-effectiveness of methane production via electrosynthesis using renewable electricity sourced from photovoltaic systems and CO_2 captured either from industrial emissions or directly from the atmosphere. Their study compared the electrochemical pathway to thermochemical, biochemical, and photoelectrochemical alternatives. They concluded that electrochemical methane production could potentially become cost-competitive with thermochemical and biochemical methods—estimated around 2.4 $/kg —only if exceptionally high-performance metrics are achieved. Specifically, current densities exceeding 5 A/cm^2 and an overall electrolyzer efficiency (encompassing both voltage and FE) greater than 50 % would be required. These conditions, however, far exceed the capabilities of current technologies. For comparison, at a more realistic performance scenario of 100 mA/cm^2 and 15 % energy efficiency, the calculated methane production cost balloons to 10.7 $/kg, underlining the present technological limitations.

From this analysis, it can be concluded that electrochemical methane production is not yet economically viable. Specifically, as already discussed in previous Sections, current electrochemical performance has not yet attained the thresholds required for reliable long-term industrial implementation, while the cost of electricity remains the predominant factor limiting large-scale deployment. Nevertheless, the substantial progress observed over the past years [12] indicates a clear trajectory of performance enhancement, and projected reductions in electricity prices further support this trend [158]. Taken together, these considerations suggest that the development of an industrial-scale system for the electrochemical conversion of CO_2 to CH_4 may become a feasible prospect within the coming decades.

9. Perspective scenario: electrochemical biogas upgrading

Despite all the challenges associated with electrochemical methane production discussed so far—ranging from low selectivity and conversion efficiencies to high energy demands and capital costs—the studies presented in the previous section collectively underscore the promising long-term potential of this technology. These investigations demonstrate that, with continued advancements in catalyst design, system integration, and energy supply strategies, electrochemical methane synthesis may become a viable alternative or complement to conventional routes, particularly in scenarios aligned with decarbonization goals and renewable energy integration. To fully unlock this potential, however, it is essential to critically evaluate the characteristics of the CO_2 feedstock employed in the process. Most of the existing studies focus on dilute or challenging carbon sources, such as CO_2 captured from flue gases, atmospheric air, or even seawater, which typically involve additional energy and infrastructure requirements for separation, purification, and compression. While these pathways are relevant in the context of direct air capture or point-source decarbonization, they often introduce technical and economic complexities that can hinder practical deployment at scale. In our view, a particularly promising and underutilized CO_2 source for electrochemical conversion is biogas.

Biogas is produced through the anaerobic digestion of organic matter, such as agricultural residues, food waste, and wastewater sludge. It consists primarily of methane (50–70 %) and carbon dioxide (30–50 %), along with trace amounts of other gases (hydrogen sulfide, water vapor, hydrogen, oxygen, nitrogen, …) [165]. While biogas is a valuable source of renewable energy, its raw composition limits its direct use in many applications, since CO_2 and trace gases reduce the heating value [166]. Therefore, upgrading biogas to biomethane, *i.e.* a purified form with higher (>95 %) methane content, has become a crucial step in maximizing its efficiency, economic viability, and environmental benefits [167]. The following subsection will report details on the technologies currently employed for biogas upgrading.

9.1. Technologies for biogas upgrading

Biogas treatment typically involves two sequential processes: cleaning and upgrading. The cleaning step focuses on the removal of trace contaminants, such as hydrogen sulphide, and other particulates, which are considered minor but potentially harmful components. This initial stage, despite often being energy-intensive, is essential for protecting equipment and ensuring compatibility with other downstream upgrading technologies. The successive upgrading process is properly aimed at increasing the methane content by selectively removing CO_2. Over the past few decades, several upgrading technologies have been extensively studied and established at industrial level. These technologies, reported in Table 3, are primarily classified based on their approach to carbon dioxide management in order to achieve a higher concentration of CH_4. The most established and efficient techniques for biogas upgrading employ CO_2 removal either exploiting the differences in physical or chemical properties between the two gases (physical/chemical scrubbing, pressure swing adsorption), or through selective separation methods (membranes, cryogenic processes).

Water (physical) scrubbing is one of the most common approaches due to its simplicity, reliability, and relatively high efficiency [168]. It takes advantage of the higher solubility of CO_2 in water compared to methane: as biogas is pressurized and passed through a water column, CO_2 is absorbed, leaving behind a high purity methane gas. However, this method requires substantial water use, as well as considerable

Table 3
Comparison of principal technologies for biogas upgrading.

Technology	CH_4 Purity	Energy Use	Maturity	Advantages	Disadvantages
Water Scrubbing	95–98 %	Medium	High	Simple, no chemicals, low cost	Water consumption, moderate CH_4 loss
PSA	>97 %	High	High	High purity, compact, fully automated	High cost, adsorbent wear, sensitive to gas quality
Membrane Separation	92–96 %	Medium	High	Modular, scalable, low maintenance	Requires multiple stages, membrane degradation
Chemical Scrubbing	>99 %	Very High	High	Excellent CO_2 removal, proven for large plants	High operational cost, chemical handling and degradation
Cryogenic Separation	>97 %	Very High	Medium	Bio-LNG production, very high purity	Complex, energy-intensive, high CAPEX
Biological Upgrading	95–98 %	Low	Medium	Low energy, mild conditions, renewable integration	Needs H_2, low reaction rates, sensitive microbiology, still maturing
Thermocatalytic	>95 %	High	Medium	Adds CH_4 yield, power-to-gas compatible	Needs H_2, catalyst degradation, higher complexity

energy and heat input for compression and water regeneration. Another common approach is chemical scrubbing, which operates on similar principles: it uses reactive solvents (typically amine- or alkaline-based) to chemically bind CO_2 in an absorption column [169]. While this method can achieve high CO_2 removal efficiencies, it relies on temperature-sensitive reactions and therefore demands repeated heating and cooling cycles for solvent regeneration, which is associated with considerable operational costs. PSA is another mature technology that separates CO_2 from methane using solid adsorbents such as activated carbon or zeolites, that selectively capture CO_2 and other trace gases under high pressure. When the pressure is reduced, the adsorbed gases are released, and the adsorbent is regenerated. PSA offers high methane purity but involves complex control systems and periodic maintenance [170]. More recent technologies include cryogenic and membrane separation. Cryogenic upgrading separates CO_2 by cooling the biogas to very low temperatures, causing CO_2 to condense or freeze while methane remains in gaseous form. This method enables the production of high-purity biomethane and has gained attention due to its ability to simultaneously produce liquefied biomethane (bio-LNG) despite being highly energy and cost-intensive [171]. Membrane based technologies instead rely on differential gas permeabilities to separate CH_4 from CO_2. While membranes are appealing for their flexibility and low maintenance, achieving very high methane purity often requires multi-step systems, and membrane degradation can occur over time due to exposure to impurities [172].

While all the above-mentioned technologies aim to remove CO_2, recent developments have shifted attention toward CO_2 utilization, particularly through methanation. These approaches convert CO_2 into additional methane, eliminating the need for CO_2 disposal and reducing greenhouse gas emissions. Biological upgrading leverages specific microorganisms, such as methanogenic archaea, that consume CO_2 and H_2 during anaerobic digestion to biologically produce methane [173,174]. If this process is conducted in-situ (directly inside the reactor), it uses the CO_2 component of biogas to reach very high methane yields. It is a low-energy, low-temperature process with potential for integration into circular bioeconomy systems but still emerging at industrial scale as it requires strict control of microbial activity and operational conditions. Thermocatalytic methanation, based on the Sabatier reaction, is another developing field with strong potential for biogas upgrading. It involves the chemical conversion of CO_2 and H_2 into methane using metal-based catalysts (such as nickel and ruthenium) at elevated temperatures (typically 300–700 °C) and pressures (10–20 bar) [175]. The main limitations are its high thermal energy demand and the sensitivity of catalysts to impurities, which can lead to degradation or deactivation over time.

9.2. Electrochemical biogas upgrading

In recent years, electrochemical methods have emerged as a promising alternative also for biomethane production, offering enhanced selectivity, energy efficiency, and potential for integration with renewable electricity sources. Electrochemical biogas upgrading represents, in fact, an innovative approach that not only purifies methane but also valorizes the separated CO_2, thereby enhancing the overall sustainability of the process.

Despite its advantages, electrochemical biogas upgrading still faces several challenges that must be addressed before large-scale deployment, including the catalyst stability and selectivity already discussed in the previous sections, and also the integration with biogas plants, since the existing infrastructure is designed for conventional upgrading methods [18]. Nevertheless, considering that, unlike flue gas or ambient air, biogas already contains a high concentration of CO_2 mixed with CH_4, using biogas as feedstock will eliminate the need for costly CO_2 capture and purification steps. In this scenario, the entire biogas stream can be directly fed into the electrolyzer, simplifying system design and reducing capital and operational expenditures, as discussed in Section 8. In particular, a 10–20 % reduction in costs can be expected thanks to the elimination of CO_2 capture and purification operations [160,161].This economic perspective has prompted the scientific community to explore the possibility of electrochemical upgrading.

In a pioneering conceptual study by Gattrell et al. [153], the productivity of an electrochemical system for upgrading biogas (composed of 60 % CH_4 and 40 % CO_2) consisting of 5 filter press flow-by reactors [176] arranged in series (each with 50 % conversion), powered by 100 mA/cm^2 and a cell voltage of 3.0 V, was calculated. A brief schematic of the analyzed system is reported in Fig. 12. Considering the use of stacked copper screens as a catalyst, an output gas composed of 73 % methane, 19 % hydrogen, and the remainder carbon monoxide, ethylene, and unreacted carbon dioxide was obtained. This led to an efficiency for the electrochemical conversion of electrical energy to chemical energy of around 38 %. Moreover, it is noteworthy that the composition of this gas mixture closely resembles that of hythane, a hydrogen–methane blend that has gained attention as a renewable fuel candidate. Hythane exhibits favorable combustion properties, such as reduced pollutant emissions and high energy efficiency, making it particularly attractive for transportation applications. Furthermore, its compatibility with existing natural gas infrastructure enhances its practicality, while its hydrogen content positions it as a strategic intermediate in the transition toward hydrogen-based energy systems [177]. An analogous outcome was experimentally demonstrated by Huang and coworkers employing an H-type cell equipped with graphite electrodes, wherein $CaSiO_3$ was dissolved in the anodic compartment, separated from the cathodic chamber by a CEM [178]. Through the electro-migration of Ca^{2+} ions toward the cathode, a fraction of the CO_2 present in the biogas feed was selectively sequestered as $CaCO_3$. Concurrently, hydrogen evolution at the cathode enabled the generation of hythane, with an outlet gas composition of approximately CH_4:H_2:CO_2 = 75:15:10 % under an applied cell potential of 3.5–4.0 V. Notably, the methane concentration in the product stream corresponded to 98–99 % of the methane fraction initially present in the biogas feed, which implies minimal methane loss compared to other upgrading methods. It is important to emphasize that this approach does not involve an actual conversion of CO_2 into methane, but simply an upgrade of biogas because the CO_2 is separated and stored in the form of bicarbonate. Similarly, Mohammadpour et al.

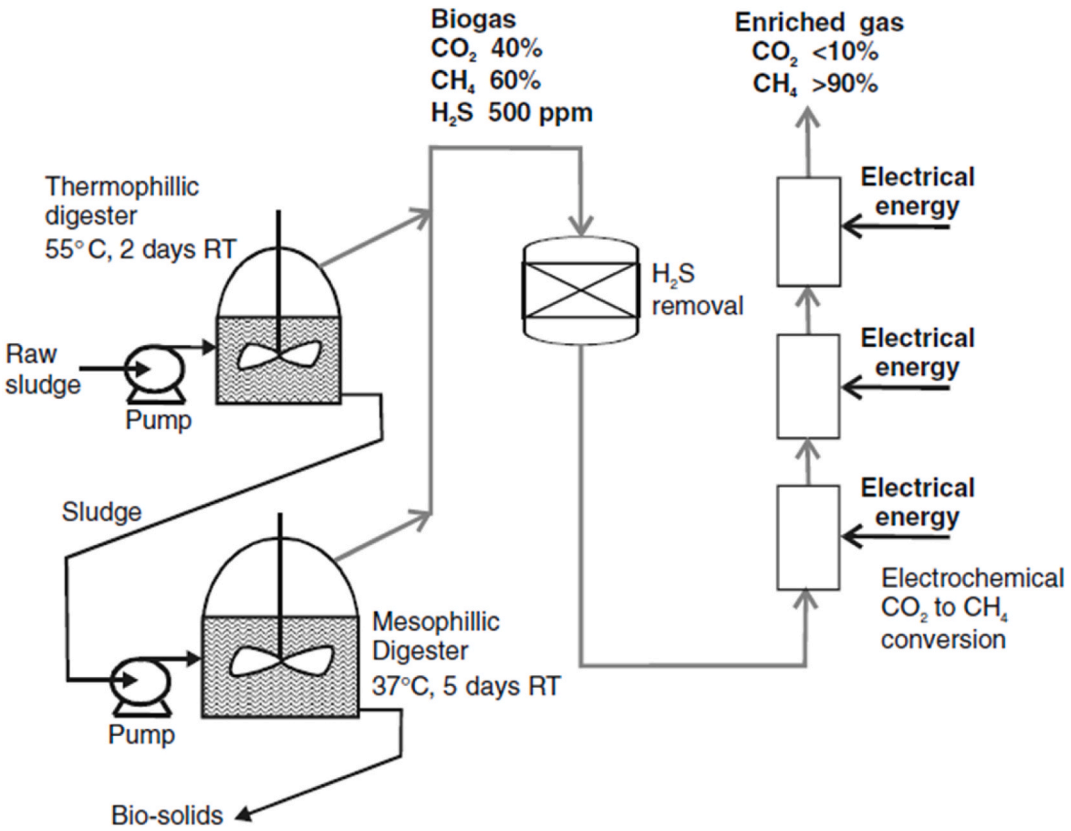

Fig. 12. Schematic of an electrochemical system for the upgrading of sewage sludge biogas. Reproduced from [153] with permission.

[179] proposed a three-chamber system, where the separation of CO_2 from CH_4 is made possible by the basification of the catholyte induced by hydrogen production, which leads to the formation of (bi)carbonate ions. These migrate (through an AEM) into the central compartment, where they react with protons from the anode (produced by OER, which pass through a CEM), thus releasing pure CO_2 gas. The cell operated for 40 h, with a current density of 30 mA/cm^2 and a voltage lower than 4 V.

Critical examination of the available literature indicates that, while the direct electrochemical conversion of CO_2 in biogas into CH_4 represents a conceptually attractive strategy for the upgrading, to the best of our knowledge no studies have yet provided experimental validation of this pathway, with the sole exception of bioelectrochemical systems [180–182], which nevertheless fall beyond the scope of the present review. This should provide the impetus for progress in research in this field. As highlighted in Welch et al. [161], future improvements in catalyst design—especially those that enhance current density—could significantly lower methane production costs. Furthermore, as discussed above, although improving FE for CH_4 is advantageous, an equally viable strategy would be to tune the electrolysis process such that hydrogen is the only byproduct. This would result in the production of hythane, that can be used directly without the need for additional downstream separation, further improving system economics [183]. A final comment regards the heavy influence of electricity cost on overall exploitability. As of now, the relatively high price of electricity remains a major barrier. However, looking toward a future where renewable energy sources become more widespread and economically accessible, the cost of green electricity is expected to decline significantly. In such a scenario, the production of low-carbon, electrochemically synthesized biomethane could become not only technically feasible but also commercially attractive, thereby playing a vital role in the transition toward a sustainable and circular energy economy.

10. Conclusions

The electrochemical reduction of CO_2 to CH_4 has gained considerable attention as a sustainable route for both carbon utilization and renewable fuel production. A bibliometric analysis of scientific publications over the past two decades shows a marked increase in research output, especially after 2013, reflecting growing interest in electrochemical carbon conversion technologies in the context of climate change mitigation and energy transition. The rise in interdisciplinary collaborations, particularly among materials scientists, chemists and engineers, highlights the complex and multifaceted nature of this field. While academic interest is accelerating, the gap between laboratory-scale success and industrial relevance remains a key challenge to address.

At the core of this process lie the catalytic materials and reactor configurations, which strongly influence selectivity, efficiency, and scalability. Copper remains the benchmark catalyst due to its unique ability to reduce CO_2 beyond CO to hydrocarbons like CH_4. Recent advances have included nanostructured copper catalysts, oxide-derived systems, and bimetallic formulations designed to stabilize key intermediates and suppress competing reactions like hydrogen evolution. Operative conditions such as electrolyte composition, temperature, pressure, and pH also play crucial roles in optimizing reaction kinetics and product distribution. Reactor designs have evolved from simple H-cells to more sophisticated flow cells and GDE systems, with MEA configurations offering higher current densities and better scalability. Nevertheless, achieving industrially relevant performance is still an ongoing endeavour. All these aspects are summarized in the sketch shown in Fig. 13.

From a practical perspective, scaling up CO_2-to-CH_4 conversion involves not only technical hurdles but also economic considerations. TEA underscores the importance of renewable electricity prices, catalyst longevity, system integration costs, and product purification in

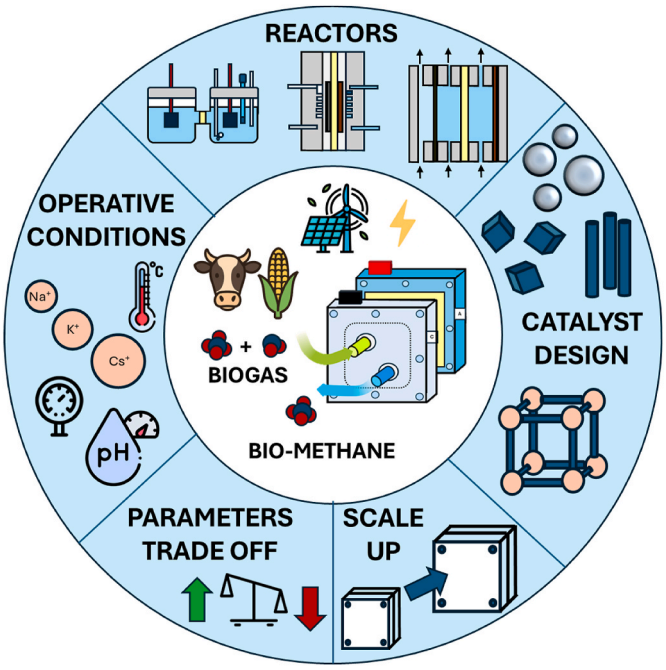

Fig. 13. Conceptual representation of the factors influencing the development of electrochemical biogas upgrading. At the core, the process couples biogas upgrading with electrochemical CO_2 conversion, offering the advantage of being directly powered by renewable electricity, thus enabling carbon-neutral or even carbon-negative energy cycles. Surrounding this central concept are the main aspects that must be addressed to achieve industrial viability: (i) catalyst and electrode design, ensuring high activity, selectivity, durability and scalability; (ii) reactor engineering and configuration, including mass transport optimization, cell architecture; (iii) operating conditions, such as pressure, temperature, electrolyte management; (iv) trade-offs among key performance indicators; (v) scaling strategies, considering techno-economic feasibility, modularity, and system robustness.

determining commercial viability. While current systems remain cost-intensive, projections suggest that with improvements in electrolyzer design and catalyst durability, costs could decrease substantially—especially if co-located with sources of concentrated CO_2 emissions or renewable energy generation. Hybridization with existing energy infrastructures, such as power-to-gas facilities or anaerobic digestion plants, may accelerate market adoption by leveraging synergies and reducing capital costs. For instance, using CO_2 from biogas upgrading units as feedstock for electroreduction could transform waste emissions into additional CH_4 output, effectively increasing overall system efficiency.

In particular, integrating electrochemical CO_2 reduction into biogas ecosystems offers a unique opportunity for enhancing methane yields while contributing to a circular carbon economy. In fact, electrochemical conversion of this CO_2 to CH_4 using surplus renewable electricity would not only improve carbon utilization but also smooth out fluctuations in biogas production tied to feedstock availability or digestion kinetics. This hybrid strategy could enable decentralized energy systems capable of producing storable methane fuel while minimizing GHG emissions. Future research should focus on pilot-scale demonstrations of such integrated platforms, supported by comprehensive lifecycle and technoeconomic assessments to validate environmental and financial sustainability under real-world conditions.

Declaration of competing interest

The authors declare the following financial interests/personal relationships which may be considered as potential competing interests: Sara Verhovez reports financial support was provided by Ministero dell'Università e della Ricerca. Adriano Sacco reports financial support was provided by Ministero dell'Università e della Ricerca. Adriano Sacco reports financial support was provided by European Commission. If there are other authors, they declare that they have no known competing financial interests or personal relationships that could have appeared to influence the work reported in this paper.

Acknowledgments

This publication is part of the project PNRR-NGEU which has received funding from the MUR – DM 630/2024. In addition, funding from EU's Horizon 2021 programme under the Marie Skłodowska-Curie Doctoral Networks (MSCA-DN) grant agreement No 101072830 (ECO-MATES) is acknowledged. Finally, this study was partially developed in the framework of the research activities carried out within the Project "Network 4 Energy Sustainable Transition—NEST", Spoke 4, Project code PE0000021, funded under the National Recovery and Resilience Plan (NRRP), Mission 4, Component 2, Investment 1.3— Call for tender No. 1561 of October 11, 2022 of Ministero dell'Università e della Ricerca (MUR); funded by the European Union—NextGenerationEU.

Data availability

Data will be made available on request.

References

[1] Abbass K, Qasim MZ, Song H, Murshed M, Mahmood H, Younis I. A review of the global climate change impacts, adaptation, and sustainable mitigation measures. Environ Sci Pollut Res 2022;29(28):42539–59. https://doi.org/10.1007/s11356-022-19718-6.

[2] Weiskopf SR, Rubenstein MA, Crozier LG, Gaichas S, Griffis R, Halofsky JE, Hyde KJW, Morelli TL, Morisette JT, Muñoz RC, Pershing AJ, Peterson DL, Poudel R, Staudinger MD, Sutton-Grier AE, Thompson L, Vose J, Weltzin JF, Whyte KP. Climate change effects on biodiversity, ecosystems, ecosystem services, and natural resource management in the United States. Sci Total Environ 2020;733:137782. https://doi.org/10.1016/j.scitotenv.2020.137782.

[3] Filonchyk M, Peterson MP, Zhang L, Hurynovich V, He Y. Greenhouse gases emissions and global climate change: examining the influence of CO2, CH4, and N2O. Sci Total Environ 2024;935:173359. https://doi.org/10.1016/j.scitotenv.2024.173359.

[4] Liu Enbin, Lu Xudong, Wang Daocheng. A systematic review of carbon capture, utilization and storage: status, progress and challenges. Energies 2023;16(6):2865.

[5] Stančin H, Mikulčić H, Wang X, Duić N. A review on alternative fuels in future energy system. Renew Sustain Energy Rev 2020;128:109927. https://doi.org/10.1016/j.rser.2020.109927.

[6] Sacco A, Speranza R, Savino U, Zeng J, Farkhondehfal MA, Lamberti A, Chiodoni A, Pirri CF. An integrated device for the solar-driven electrochemical conversion of CO2 to CO. ACS Sustainable Chem Eng 2020;8(20):7563–8. https://doi.org/10.1021/acssuschemeng.0c02088.

[7] Agliuzza M, Mezza A, Sacco A. Solar-Driven integrated carbon capture and utilization: coupling CO2 electroreduction toward CO with capture or photovoltaic systems. Appl Energy 2023;334:120649. https://doi.org/10.1016/j.apenergy.2023.120649.

[8] Jiang Y, Wang K, Wang Y, Liu Z, Gao X, Zhang J, Ma Q, Fan S, Zhao T-S, Yao M. Recent advances in thermocatalytic hydrogenation of carbon dioxide to light olefins and liquid fuels via modified fischer-tropsch pathway. J CO2 Util 2023;67:102321. https://doi.org/10.1016/j.jcou.2022.102321.

[9] Karishma S, Kamalesh R, Saravanan A, Deivayanai VC, Yaashikaa PR, Vickram AS. A review on recent advancements in biochemical fixation and transformation of CO2 into constructive products. Biochem Eng J 2024;208:109366. https://doi.org/10.1016/j.bej.2024.109366.

[10] Qiao J, Liu Y, Hong F, Zhang J. A review of catalysts for the electroreduction of carbon dioxide to produce low-carbon fuels. Chem Soc Rev 2014;43(2):631–75. https://doi.org/10.1039/C3CS60323G.

[11] Leonzio G, Hankin A, Shah N. CO2 electrochemical reduction: a state-of-the-art review with economic and environmental analyses. Chem Eng Res Des 2024;208:934–55. https://doi.org/10.1016/j.cherd.2024.07.014.

[12] Huang F, Sun H, He S, Chen X, Wei D, Xu A, Wang B, Yin X, Xu J, He H. Progress and perspectives for efficient electrochemical carbon dioxide reduction to methane. ChemSusChem 2025;18(12):e202402568. https://doi.org/10.1002/cssc.202402568.

[13] van der Zwaan B, Detz R, Meulendijks N, Buskens P. Renewable natural gas as climate-neutral energy carrier? Fuel 2022;311:122547. https://doi.org/10.1016/j.fuel.2021.122547.

[14] Burdyny T, Mulder FM. Scale-up of CO2 and CO electrolyzers. Joule 2024;8(9):2449–52. https://doi.org/10.1016/j.joule.2024.08.010.

[15] Han J, Bai X, Xu X, Bai X, Husile A, Zhang S, Qi L, Guan J. Advances and challenges in the electrochemical reduction of carbon dioxide. Chem Sci 2024;15(21):7870–907. https://doi.org/10.1039/D4SC01931H.

[16] Barecka MH, Ager JW, Lapkin AA. Techno-Economic assessment of emerging CO2 electrolysis technologies. STAR Protoc 2021;2(4):100889. https://doi.org/10.1016/j.xpro.2021.100889.

[17] Matsuda S, Osawa M, Umeda M. Progress of CO2 electrochemical methanation using a membrane electrode assembly. Electrocatalysis 2024;15(4):318–28. https://doi.org/10.1007/s12678-024-00873-y.

[18] Biswas R, Ahmadi V, Ummethala R, Mozumder MSI, Aryal N. Recent advances in electrochemical carbon dioxide reduction strategies in biogas upgrading and biomethane production. Chem Eng J Adv 2025;22:100722. https://doi.org/10.1016/j.ceja.2025.100722.

[19] Van Eck NJ, Waltman L. Software survey: vosviewer, a Computer Program for bibliometric mapping. Scientometrics 2010;84(2):523–38.

[20] Aria Massimo, Cuccurullo Corrado. Bibliometrix: an R-Tool for comprehensive science mapping analysis. J Informetr 2017;11(4):959–75.

[21] Cai J, Zhao Q, Hsu W-Y, Choi C, Liu Y, Martirez JMP, Chen C, Huang J, Carter EA, Huang Y. Highly selective electrochemical reduction of CO2 into methane on nanotwinned Cu. J Am Chem Soc 2023;145(16):9136–43. https://doi.org/10.1021/jacs.3c00847.

[22] Mosali VSS, Puxty G, Horne MD, Bond AM, Zhang J. Selective electrochemical methanation of carbon dioxide using a sulphide derived CuZn catalyst. Electrochim Acta 2024;475:143628. https://doi.org/10.1016/j.electacta.2023.143628.

[23] Weng Z, Wu Y, Wang M, Jiang J, Yang K, Huo S, Wang X-F, Ma Q, Brudvig GW, Batista VS, Liang Y, Feng Z, Wang H. Active sites of copper-complex catalytic materials for electrochemical carbon dioxide reduction. Nat Commun 2018;9(1):415. https://doi.org/10.1038/s41467-018-02819-7.

[24] Hori Y, Wakebe H, Tsukamoto T, Koga O. Adsorption of CO accompanied with simultaneous charge transfer on copper single crystal electrodes related with electrochemical reduction of CO2 to hydrocarbons. Surf Sci 1995;335:258–63. https://doi.org/10.1016/0039-6028(95)00441-6.

[25] Kaneco S, Katsumata H, Suzuki T, Ohta K. Electrochemical reduction of CO2 to methane at the Cu electrode in methanol with sodium supporting salts and its comparison with other alkaline salts. Energy Fuels 2006;20(1):409–14. https://doi.org/10.1021/ef050274d.

[26] Wang Zhijiang, Yuan Qi, Shan Jingjing, Jiang Zhaohua, Xu Ping, Hu Yongfeng, Zhou Jigang, Wu Lina, Niu Zhuangzhuang, Sun Jianmin, Cheng Tao, Goddard William A. Highly selective electrocatalytic reduction of CO2 into methane on Cu–Bi nanoalloys. J Phys Chem Lett 2020;11(17):7261–6. https://doi.org/10.1021/acs.jpclett.0c01261.

[27] Salehi M, Al-Mahayni H, Farzi A, McKee M, Kaviani S, Pajootan E, Lin R, Kornienko N, Seifitokaldani A. Copper nanoclusters: selective CO2 to Methane Conversion beyond 1 A/Cm^2. Appl Catal B Environ Energy 2024;353:124061. https://doi.org/10.1016/j.apcatb.2024.124061.

[28] Sedighian Rasouli A, Wang X, Wicks J, Lee G, Peng T, Li F, McCallum C, Dinh CT, Ip AH, Sinton D, Sargent EH. CO2 electroreduction to methane at production rates exceeding 100 mA/cm2. ACS Sustain. Chem. Eng. 2020;8(39):14668–73. https://doi.org/10.1021/acssuschemeng.0c03453.

[29] Sedighian Rasouli A, Wang X, Wicks J, Dinh C-T, Abed J, Wu F-Y, Hung S-F, Bertens K, Huang JE, Sargent EH. Ga doping disrupts C-C coupling and promotes methane electroproduction on CuAl catalysts. Chem Catal 2022;2(4):908–16. https://doi.org/10.1016/j.checat.2022.03.016.

[30] Liu J, Li P, Bi J, Jia S, Wang Y, Kang X, Sun X, Zhu Q, Han B. Switching between C2+ products and CH4 in CO2 electrolysis by tuning the composition and structure of Rare-Earth/Copper catalysts. J Am Chem Soc 2023;145(42):23037–47. https://doi.org/10.1021/jacs.3c05562.

[31] Hung S-F, Xu A, Wang X, Li F, Hsu S-H, Li Y, Wicks J, Cervantes EG, Rasouli AS, Li YC, Luo M, Nam D-H, Wang N, Peng T, Yan Y, Lee G, Sargent EH. A metal-supported single-atom catalytic site enables carbon dioxide hydrogenation. Nat Commun 2022;13(1):819. https://doi.org/10.1038/s41467-022-28456-9.

[32] Zhou X, Shan J, Chen L, Xia BY, Ling T, Duan J, Jiao Y, Zheng Y, Qiao S-Z. Stabilizing Cu2+ ions by solid solutions to promote CO2 electroreduction to methane. J Am Chem Soc 2022;144(5):2079–84. https://doi.org/10.1021/jacs.1c12212.

[33] Wang X, Ou P, Wicks J, Xie Y, Wang Y, Li J, Tam J, Ren D, Howe JY, Wang Z, Ozden A, Finfrock YZ, Xu Y, Li Y, Rasouli AS, Bertens K, Ip AH, Graetzel M, Sinton D, Sargent EH. Gold-in-Copper at low *CO coverage enables efficient electromethanation of CO2. Nat Commun 2021;12(1):3387. https://doi.org/10.1038/s41467-021-23699-4.

[34] Yang K, Kas R, Smith WA, Burdyny T. Role of the carbon-based gas diffusion layer on flooding in a gas diffusion electrode cell for electrochemical CO2 reduction. ACS Energy Lett 2021;6(1):33–40. https://doi.org/10.1021/acsenergylett.0c02184.

[35] Wu Y, Rabiee H, Song Zhao X, Wang G, Jiang Y. Insights into electrolyte flooding in flexible gas diffusion electrodes for CO 2 electrolysis: from mechanisms to effective mitigation strategies. J Mater Chem A 2024;12(24):14206–28. https://doi.org/10.1039/D4TA01994F.

[36] Leonard ME, Clarke LE, Forner-Cuenca A, Brown SM, Brushett FR. Investigating electrode flooding in a flowing electrolyte, gas-fed carbon dioxide electrolyzer. ChemSusChem 2020;13(2):400–11. https://doi.org/10.1002/cssc.201902547.

[37] Choi W, Chae Y, Liu E, Kim D, Drisdell WS, Oh H, Koh JH, Lee DK, Lee U, Won DH. Exploring the influence of cell configurations on Cu Catalyst reconstruction during CO2 electroreduction. Nat Commun 2024;15(1):8345. https://doi.org/10.1038/s41467-024-52692-w.

[38] Jin Z, Guo Y, Qiu C. Electro-Conversion of carbon dioxide to valuable chemicals in a membrane electrode assembly. Sustainability 2022;14(9):5579. https://doi.org/10.3390/su14095579.

[39] Sassenburg M, Kelly M, Subramanian S, Smith WA, Burdyny T. Zero-Gap electrochemical CO2 reduction cells: challenges and operational strategies for prevention of salt precipitation. ACS Energy Lett 2023;8(1):321–31. https://doi.org/10.1021/acsenergylett.2c01885.

[40] Li M, Idros MN, Wu Y, Burdyny T, Garg S, Zhao XS, Wang G, Rufford TE. The role of electrode wettability in electrochemical reduction of carbon dioxide. J Mater Chem A 2021;9(35):19369–409. https://doi.org/10.1039/D1TA03636J.

[41] Zhao P, Jiang H, Shen H, Yang S, Gao R, Guo Y, Zhang Q, Zhang H. Construction of low-coordination Cu−C2 single-atoms electrocatalyst facilitating the efficient electrochemical CO2 reduction to methane. Angew Chem Int Ed 2023;62(49):e202314121. https://doi.org/10.1002/anie.202314121.

[42] Wu Y, Chen C, Yan X, Wu R, Liu S, Ma J, Zhang J, Liu Z, Xing X, Wu Z, Han B. Enhancing CO2 electroreduction to CH4 over Cu nanoparticles supported on N-Doped carbon. Chem Sci 2022;13(28):8388–94. https://doi.org/10.1039/D2SC02222B.

[43] Xu Y, Li F, Xu A, Edwards JP, Hung S-F, Gabardo CM, O'Brien CP, Liu S, Wang X, Li Y, Wicks J, Miao RK, Liu Y, Li J, Huang JE, Abed J, Wang Y, Sargent EH, Sinton D. Low coordination number copper catalysts for electrochemical CO2 methanation in a membrane electrode assembly. Nat Commun 2021;12(1):2932. https://doi.org/10.1038/s41467-021-23065-4.

[44] Dai Y, Li H, Wang C, Xue W, Zhang M, Zhao D, Xue J, Li J, Luo L, Liu C, Li X, Cui P, Jiang Q, Zheng T, Gu S, Zhang Y, Xiao J, Xia C, Zeng J. Manipulating local coordination of copper single Atom catalyst enables efficient CO2-to-CH4 conversion. Nat Commun 2023;14(1):3382. https://doi.org/10.1038/s41467-023-39048-6.

[45] Lees EW, Liu A, Bui JC, Ren S, Weber AZ, Berlinguette CP. Electrolytic methane production from reactive carbon solutions. ACS Energy Lett 2022;7(5):1712–8. https://doi.org/10.1021/acsenergylett.2c00283.

[46] Obasanjo CA, Gao G, Crane J, Golovanova V, García de Arquer FP, Dinh C-T. High-Rate and selective Conversion of CO2 from aqueous solutions to hydrocarbons. Nat Commun 2023;14(1):3176. https://doi.org/10.1038/s41467-023-38963-y.

[47] Hori Y, Kikuchi K, Suzuki S. Production OF CO and CH4 IN electrochemical reduction OF CO2 at metal electrodes in aqueous hydrogencarbonate solution. Chem Lett 1985;14(11):1695–8. https://doi.org/10.1246/cl.1985.1695.

[48] Hori Y, Murata A, Takahashi R, Suzuki S. Electroreduction of CO to CH4and C2H4at a copper electrode in aqueous solutions at ambient temperature and pressure. J Am Chem Soc 1987;109(16):5022–3. https://doi.org/10.1021/ja00250a044.

[49] Kuhl KP, Cave ER, Abram DN, Jaramillo TF. New insights into the electrochemical reduction of carbon dioxide on metallic copper surfaces. Energy Environ Sci 2012;5(5):7050–9. https://doi.org/10.1039/C2EE21234J.

[50] Ren D, Fong J, Yeo BS. The effects of currents and potentials on the selectivities of copper toward carbon dioxide electroreduction. Nat Commun 2018;9(1):925. https://doi.org/10.1038/s41467-018-03286-w.

[51] Peterson AA, Abild-Pedersen F, Studt F, Rossmeisl J, Nørskov JK. How copper catalyzes the electroreduction of carbon dioxide into hydrocarbon fuels. Energy Environ Sci 2010;3(9):1311–5. https://doi.org/10.1039/C0EE00071J.

[52] Nie X, Esopi MR, Janik MJ, Asthagiri A. Selectivity of CO2 reduction on copper electrodes: the role of the kinetics of elementary steps. Angew Chem Int Ed 2013;52(9):2459–62. https://doi.org/10.1002/anie.201208320.

[53] Schouten KJP, Kwon Y, Ham C J M van der, Qin Z, Koper MTM. A new mechanism for the selectivity to C1 and C2 species in the electrochemical reduction of carbon dioxide on copper electrodes. Chem Sci 2011;2(10):1902–9. https://doi.org/10.1039/C1SC00277E.

[54] Schouten KJP, Qin Z, Pérez Gallent E, Koper MTM. Two pathways for the formation of ethylene in CO reduction on single-crystal copper electrodes. J Am Chem Soc 2012;134(24):9864–7. https://doi.org/10.1021/ja302668n.

[55] Lai Y, Watkins NB, Rosas-Hernández A, Thevenon A, Heim GP, Zhou L, Wu Y, Peters JC, Gregoire JM, Agapie T. Breaking scaling relationships in CO_2 reduction on copper alloys with organic additives. ACS Cent Sci 2021;7(10):1756–62. https://doi.org/10.1021/acscentsci.1c00860.

[56] Liu X, Xiao J, Peng H, Hong X, Chan K, Nørskov JK. Understanding trends in electrochemical carbon dioxide reduction rates. Nat Commun 2017;8(1):15438. https://doi.org/10.1038/ncomms15438.

[57] Cheng T, Xiao H, Goddard WA. Full atomistic reaction mechanism with kinetics for CO reduction on Cu(100) from Ab initio molecular dynamics free-energy calculations at 298 K. Proc Natl Acad Sci 2017;114(8):1795–800. https://doi.org/10.1073/pnas.1612106114.

[58] Zhan C, Dattila F, Rettenmaier C, Herzog A, Herran M, Wagner T, Scholten F, Bergmann A, López N, Roldan Cuenya B. Key intermediates and Cu active sites for CO2 electroreduction to ethylene and ethanol. Nat Energy 2024;9(12):1485–96. https://doi.org/10.1038/s41560-024-01633-4.

[59] Takahashi I, Koga O, Hoshi N, Hori Y. Electrochemical Reduction of CO2 at Copper Single Crystal Cu(S)-[n(111) × (111)] and Cu(S)-[n(110) × (100)] electrodes. J Electroanal Chem 2002;533(1–2):135–43. https://doi.org/10.1016/S0022-0728(02)01081-1.

[60] Hori Y, Takahashi I, Koga O, Hoshi N. Electrochemical reduction of carbon dioxide at various series of copper single crystal electrodes. J Mol Catal Chem 2003;199(1–2):39–47. https://doi.org/10.1016/S1381-1169(03)00016-5.

[61] De Gregorio GL, Burdyny T, Loiudice A, Iyengar P, Smith WA, Buonsanti R. Facet-Dependent selectivity of Cu catalysts in electrochemical CO2 reduction at

commercially viable Current densities. ACS Catal 2020;10(9):4854–62. https://doi.org/10.1021/acscatal.0c00297.
[62] Ou L, He Z. Mechanism for CO2 electroreduction into C2 products at the low overpotential: theoretical insights from an improved Electrode/Solution interface model. Surf Sci 2021;705:121782. https://doi.org/10.1016/j.susc.2020.121782.
[63] Schouten KJP, Pérez Gallent E, Koper MTM. Structure sensitivity of the electrochemical reduction of carbon monoxide on copper single crystals. ACS Catal 2013;3(6):1292–5. https://doi.org/10.1021/cs4002404.
[64] Zhang G, Zhao Z-J, Cheng D, Li H, Yu J, Wang Q, Gao H, Guo J, Wang H, Ozin GA, Wang T, Gong J. Efficient CO2 electroreduction on facet-selective copper films with high conversion rate. Nat Commun 2021;12(1):5745. https://doi.org/10.1038/s41467-021-26053-w.
[65] Durand WJ, Peterson AA, Studt F, Abild-Pedersen F, Nørskov JK. Structure effects on the energetics of the electrochemical reduction of CO2 by copper surfaces. Surf Sci 2011;605(15–16):1354–9. https://doi.org/10.1016/j.susc.2011.04.028.
[66] Vollmer S, Witte G, Wöll C. Determination of site specific adsorption energies of CO on copper. Catal Lett 2001;77(1):97–101. https://doi.org/10.1023/A:1012755616064.
[67] Shi C, Hansen HA, Lausche AC, Nørskov JK. Trends in electrochemical CO2 reduction activity for open and close-packed metal surfaces. Phys Chem Chem Phys 2014;16(10):4720–7. https://doi.org/10.1039/C3CP54822H.
[68] Tang W, Peterson AA, Varela AS, Jovanov ZP, Bech L, Durand WJ, Dahl S, Nørskov JK, Chorkendorff I. The importance of surface morphology in controlling the selectivity of polycrystalline copper for CO2 electroreduction. Phys Chem Chem Phys 2011;14(1):76–81. https://doi.org/10.1039/C1CP22700A.
[69] Scholten F, Nguyen K-LC, Bruce JP, Heyde M, Roldan Cuenya B. Identifying structure–selectivity correlations in the electrochemical reduction of CO2: a comparison of well-ordered atomically clean and chemically etched copper single-crystal surfaces. Angew Chem Int Ed 2021;60(35):19169–75. https://doi.org/10.1002/anie.202103102.
[70] Choi C, Cai J, Lee C, Lee HM, Xu M, Huang Y. Intimate atomic Cu-Ag interfaces for high CO2RR selectivity towards CH4 at low over potential. Nano Res 2021;14(10):3497–501. https://doi.org/10.1007/s12274-021-3639-x.
[71] Guo P, Liu K, Liu X, Liu R, Yin Z. Perspectives on Cu–Ag bimetallic catalysts for electrochemical CO_2 reduction reaction: a mini-review. Energy Fuels 2024;38(7):5659–75. https://doi.org/10.1021/acs.energyfuels.3c05194.
[72] Feng Y, An W, Wang Z, Wang Y, Men Y, Du Y. Electrochemical CO2 reduction reaction on M@Cu(211) bimetallic single-atom surface alloys: mechanism, kinetics, and catalyst screening. ACS Sustainable Chem Eng 2020;8(1):210–22. https://doi.org/10.1021/acssuschemeng.9b05183.
[73] Wang R, Jiang R, Dong C, Tong T, Li Z, Liu H, Du X-W. Engineering a Cu/ZnOx interface for high methane selectivity in CO2 electrochemical reduction. Ind Eng Chem Res 2021;60(1):273–80. https://doi.org/10.1021/acs.iecr.0c04718.
[74] Kuhl KP, Hatsukade T, Cave ER, Abram DN, Kibsgaard J, Jaramillo TF. Electrocatalytic conversion of carbon dioxide to methane and methanol on transition metal surfaces. J Am Chem Soc 2014;136(40):14107–13. https://doi.org/10.1021/ja505791r.
[75] Zhang H, Chang X, Chen JG, Goddard WA, Xu B, Cheng M-J, Lu Q. Computational and experimental demonstrations of one-pot tandem catalysis for electrochemical carbon dioxide reduction to methane. Nat Commun 2019;10(1):3340. https://doi.org/10.1038/s41467-019-11292-9.
[76] Reske R, Mistry H, Behafarid F, Roldan Cuenya B, Strasser P. Particle size effects in the catalytic electroreduction of CO2 on Cu nanoparticles. J Am Chem Soc 2014;136(19):6978–86. https://doi.org/10.1021/ja500328k.
[77] Iyengar P, Huang J, Gregorio GLD, Gadiyar C, Buonsanti R. Size dependent selectivity of Cu Nano-Octahedra catalysts for the electrochemical reduction of CO2 to CH4. Chem Commun 2019;55(60):8796–9. https://doi.org/10.1039/C9CC02522G.
[78] Roldan Cuenya B. Metal nanoparticle catalysts beginning to Shape-Up. Acc Chem Res 2013;46(8):1682–91. https://doi.org/10.1021/ar300226p.
[79] Li Y, Cui F, Ross MB, Kim D, Sun Y, Yang P. Structure-Sensitive CO2 electroreduction to hydrocarbons on ultrathin 5-Fold twinned copper nanowires. Nano Lett 2017;17(2):1312–7. https://doi.org/10.1021/acs.nanolett.6b05287.
[80] Weng Z, Jiang J, Wu Y, Wu Z, Guo X, Materna KL, Liu W, Batista VS, Brudvig GW, Wang H. Electrochemical CO2 reduction to hydrocarbons on a heterogeneous molecular Cu catalyst in aqueous solution. J Am Chem Soc 2016;138(26):8076–9. https://doi.org/10.1021/jacs.6b04746.
[81] Loiudice A, Lobaccaro P, Kamali EA, Thao T, Huang BH, Ager JW, Buonsanti R. Tailoring copper nanocrystals towards C2 products in electrochemical CO2 reduction. Angew Chem Int Ed 2016;55(19):5789–92. https://doi.org/10.1002/anie.201601582.
[82] Roberts FS, Kuhl KP, Nilsson A. High selectivity for ethylene from carbon dioxide reduction over copper nanocube electrocatalysts. Angew Chem Int Ed 2015;54(17):5179–82. https://doi.org/10.1002/anie.201412214.
[83] Wang Z, Yang G, Zhang Z, Jin M, Yin Y. Selectivity on etching: creation of high-energy facets on copper nanocrystals for CO2 electrochemical reduction. ACS Nano 2016;10(4):4559–64. https://doi.org/10.1021/acsnano.6b00602.
[84] Rossi K, Buonsanti R. Shaping copper nanocatalysts to steer selectivity in the electrochemical CO2 reduction reaction. Acc Chem Res 2022;55(5):629–37. https://doi.org/10.1021/acs.accounts.1c00673.
[85] Manthiram K, Beberwyck BJ, Alivisatos AP. Enhanced electrochemical methanation of carbon dioxide with a dispersible nanoscale copper catalyst. J Am Chem Soc 2014;136(38):13319–25. https://doi.org/10.1021/ja5065284.
[86] Zhang J, Pham THM, Gao Z, Li M, Ko Y, Lombardo L, Zhao W, Luo W, Züttel A. Electrochemical CO_2 reduction over copper phthalocyanine derived catalysts with enhanced selectivity for multicarbon products. ACS Catal. 2023;13(14):9326–35. https://doi.org/10.1021/acscatal.3c01439.
[87] Hu Q, Han Z, Wang X, Li G, Wang Z, Huang X, Yang H, Ren X, Zhang Q, Liu J, He C. Facile synthesis of sub-nanometric copper clusters by double confinement enables selective reduction of carbon dioxide to methane. Angew Chem Int Ed 2020;59(43):19054–9. https://doi.org/10.1002/anie.202009277.
[88] Bai H, Cheng T, Li S, Zhou Z, Yang H, Li J, Xie M, Ye J, Ji Y, Li Y, Zhou Z, Sun S, Zhang B, Peng H. Controllable CO adsorption determines ethylene and methane productions from CO2 electroreduction. Sci Bull 2021;66(1):62–8. https://doi.org/10.1016/j.scib.2020.06.023.
[89] Ma M, Djanashvili K, Smith WA. Controllable hydrocarbon formation from the electrochemical reduction of CO2 over Cu Nanowire arrays. Angew Chem Int Ed 2016;55(23):6680–4. https://doi.org/10.1002/anie.201601282.
[90] Dai H, Song T, Yue X, Wei S, Li F, Xu Y, Shu S, Cui Z, Wang C, Gu J, Duan L. Cu single-atom electrocatalyst on nitrogen-containing graphdiyne for CO2 electroreduction to CH4. Chin J Catal 2024;64:123–32. https://doi.org/10.1016/S1872-2067(24)60106-3.
[91] Shi G, Xie Y, Du L, Fu X, Chen X, Xie W, Lu T-B, Yuan M, Wang M. Constructing cu−c bonds in a graphdiyne-regulated Cu single-atom electrocatalyst for CO2 reduction to CH4. Angew Chem Int Ed 2022;61(23):e202203569. https://doi.org/10.1002/anie.202203569.
[92] Cai Y, Fu J, Zhou Y, Chang Y-C, Min Q, Zhu J-J, Lin Y, Zhu W. Insights on forming N,O-Coordinated Cu single-atom catalysts for electrochemical reduction CO2 to methane. Nat Commun 2021;12(1):586. https://doi.org/10.1038/s41467-020-20769-x.
[93] Wei S, Jiang X, He C, Wang S, Hu Q, Chai X, Ren X, Yang H, He C. Construction of single-atom copper sites with low coordination number for efficient CO2 electroreduction to CH4. J Mater Chem A 2022;10(11):6187–92. https://doi.org/10.1039/D1TA08494A.
[94] Burwell T, Thangamuthu M, Aliev GN, Ghaderzadeh S, Kohlrausch EC, Chen Y, Theis W, Norman LT, Fernandes JA, Besley E, Licence P, Khlobystov AN. Direct Formation of copper nanoparticles from atoms at graphitic step edges lowers overpotential and improves selectivity of electrocatalytic CO2 reduction. Commun Chem 2024;7(1):1–10. https://doi.org/10.1038/s42004-024-01218-y.
[95] Roy S, Li Z, Chen Z, Mata AC, Kumar P, Sarma S Ch, Teixeira IF, Silva IF, Gao G, Tarakina NV, Kibria MG, Singh CV, Wu J, Ajayan PM. Cooperative copper single-atom catalyst in 2D carbon nitride for enhanced CO2 electrolysis to methane. Adv Mater 2024;36(13):2300713. https://doi.org/10.1002/adma.202300713.
[96] Wang Y-R, Liu M, Gao G-K, Yang Y-L, Yang R-X, Ding H-M, Chen Y, Li S-L, Lan Y-Q. Implanting numerous hydrogen-bonding networks in a cu-porphyrin-based nanosheet to boost CH4 selectivity in neutral-media CO2 electroreduction. Angew Chem Int Ed 2021;60(40):21952–8. https://doi.org/10.1002/anie.202108388.
[97] Yu P, Lv X, Wang Q, Huang H, Weng W, Peng C, Zhang L, Zheng G. Promoting electrocatalytic CO2 reduction to CH4 by copper porphyrin with donor–acceptor structures. Small 2023;19(4):2205730. https://doi.org/10.1002/smll.202205730.
[98] Li Q, Wang Z-M, Chen Y, Wang Y-R, Guo C, Huang Q, Dong L-Z, Li S-L, Lan Y-Q. CO2-to-CH4 electroreduction over scalable Cu-Porphyrin based organic polymers promoted by direct auxiliary bonding interaction. J Mater Chem A 2022;10(47):25356–62. https://doi.org/10.1039/D2TA05934G.
[99] Cao W, Yang D, Li B, Mi Y, Qi K, Mao Y, Zhao Y, Li H, He Z-H. Porphyrin-Based metal–organic frameworks anchored with Cu species for highly efficient electrocatalytic CO2 reduction to CH4. Green Chem 2025. https://doi.org/10.1039/D5GC02085A.
[100] Guan A, Chen Z, Quan Y, Peng C, Wang Z, Sham T-K, Yang C, Ji Y, Qian L, Xu X, Zheng G. Boosting CO2 electroreduction to CH4 via tuning neighboring single-copper sites. ACS Energy Lett 2020;5(4):1044–53. https://doi.org/10.1021/acsenergylett.0c00018.
[101] Lee SH, Lin JC, Farmand M, Landers AT, Feaster JT, Avilés Acosta JE, Beeman JW, Ye Y, Yano J, Mehta A, Davis RC, Jaramillo TF, Hahn C, Drisdell WS. Oxidation State and surface reconstruction of Cu under CO2 reduction conditions from in situ X-Ray characterization. J Am Chem Soc 2021;143(2):588–92. https://doi.org/10.1021/jacs.0c10017.
[102] Li Y, Kim D, Louisia S, Xie C, Kong Q, Yu S, Lin T, Aloni S, Fakra SC, Yang P. Electrochemically scrambled nanocrystals are catalytically active for CO2-to-Multicarbons. Proc Natl Acad Sci 2020;117(17):9194–201. https://doi.org/10.1073/pnas.1918602117.
[103] Fan Q, Zhang X, Ge X, Bai L, He D, Qu Y, Kong C, Bi J, Ding D, Cao Y, Duan X, Wang J, Yang J, Wu Y. Manipulating Cu nanoparticle surface oxidation States tunes catalytic selectivity toward CH4 or C2+ products in CO2 electroreduction. Adv Energy Mater 2021;11(36):2101424. https://doi.org/10.1002/aenm.202101424.
[104] De Luna P, Quintero-Bermudez R, Dinh C-T, Ross MB, Bushuyev OS, Todorović P, Regier T, Kelley SO, Yang P, Sargent EH. Catalyst electro-redeposition controls morphology and oxidation State for selective carbon dioxide reduction. Nat Catal 2018;1(2):103–10. https://doi.org/10.1038/s41929-017-0018-9.
[105] Wang J, Tan H-Y, Zhu Y, Chu H, Chen HM. Linking the dynamic chemical State of catalysts with the product profile of electrocatalytic CO2 reduction. Angew Chem Int Ed 2021;60(32):17254–67. https://doi.org/10.1002/anie.202017181.
[106] Chou T-C, Chang C-C, Yu H-L, Yu W-Y, Dong C-L, Velasco-Vélez J-J, Chuang C-H, Chen L-C, Lee J-F, Chen J-M, Wu H-L. Controlling the oxidation State of the Cu electrode and reaction intermediates for electrochemical CO_2 reduction to ethylene. J Am Chem Soc 2020;142(6):2857–67. https://doi.org/10.1021/jacs.9b11126.
[107] Chen X, Jia S, Chen C, Jiao J, Zhai J, Deng T, Xue C, Cheng H, Dong M, Xia W, Zeng J, Xing X, Wu H, He M, Han B. Highly stable layered coordination polymer

electrocatalyst toward efficient CO2-to-CH4 conversion. Adv Mater 2024;36(11): 2310273. https://doi.org/10.1002/adma.202310273.
[108] Zhang Y, Dong L-Z, Li S, Huang X, Chang J-N, Wang J-H, Zhou J, Li S-L, Lan Y-Q. Coordination environment dependent selectivity of single-site-cu enriched crystalline porous catalysts in CO2 reduction to CH4. Nat Commun 2021;12(1): 6390. https://doi.org/10.1038/s41467-021-26724-8.
[109] Liu Y, Li S, Dai L, Li J, Lv J, Zhu Z, Yin A, Li P, Wang B. The synthesis of Hexaazatrinaphthylene-Based 2D conjugated copper metal-organic framework for highly selective and stable electroreduction of CO2 to methane. Angew Chem Int Ed 2021;60(30):16409–15. https://doi.org/10.1002/anie.202105966.
[110] Hori Y. Electrochemical CO2 reduction on metal electrodes. In: Vayenas CG, White RE, Gamboa-Aldeco ME, editors. Modern aspects of electrochemistry. New York, NY: Springer; 2008. p. 89–189. https://doi.org/10.1007/978-0-387-49489-0_3.
[111] Nitopi S, Bertheussen E, Scott SB, Liu X, Engstfeld AK, Horch S, Seger B, Stephens IEL, Chan K, Hahn C, Nørskov JK, Jaramillo TF, Chorkendorff I. Progress and perspectives of electrochemical CO_2 reduction on copper in aqueous electrolyte. Chem Rev 2019;119(12):7610–72. https://doi.org/10.1021/acs.chemrev.8b00705.
[112] Umeda M, Niitsuma Y, Horikawa T, Matsuda S, Osawa M. Electrochemical reduction of CO2 to methane on platinum catalysts without overpotentials: strategies for improving conversion efficiency. ACS Appl Energy Mater 2020;3(1): 1119–27. https://doi.org/10.1021/acsaem.9b02178.
[113] Matsuda S, Yoshida Y, Umeda M. Electroreduction of CO to CH without overpotential using Pt-Black catalysts: enhancement of faradaic efficiency. Int J Energy Res 2022;46(7):9919–25. https://doi.org/10.1002/er.7836.
[114] Yang H, Cai H, Li D, Kong Y, Feng S, Jiang X, Hu Q, He C. Molecular modification enables CO2 electroreduction to methane on platinum surface in acidic media. Natl Sci Rev 2024;11(12):nwae361. https://doi.org/10.1093/nsr/nwae361.
[115] Zheng M, Zhou X, Wang Y, Chen G, Li M. The facet dependence of CO2 electroreduction selectivity on a Pd3Au bimetallic catalyst: a DFT Study. Molecules 2023;28(7):3169. https://doi.org/10.3390/molecules28073169.
[116] Klinkova A, De Luna P, Dinh C-T, Voznyy O, Larin EM, Kumacheva E, Sargent EH. Rational design of efficient palladium catalysts for electroreduction of carbon dioxide to formate. ACS Catal 2016;6(12):8115–20. https://doi.org/10.1021/acscatal.6b01719.
[117] Back S, Jung Y. TiC- and TiN-Supported single-atom catalysts for dramatic improvements in CO2 electrochemical reduction to CH4. ACS Energy Lett 2017;2 (5):969–75. https://doi.org/10.1021/acsenergylett.7b00152.
[118] Wu R, Liu D, Geng J, Bai H, Li F, Zhou P, Pan H. Electrochemical reduction of CO2 on single-atom catalysts anchored on N-Terminated TiN (1 1 1): low overpotential and high selectivity. Appl Surf Sci 2022;602:154239. https://doi.org/10.1016/j.apsusc.2022.154239.
[119] Ma Y, Hao J, Jia B, Zhang X, Zhang C, Wu G, Chen C, Li Y, Zhou Z, Li Q, Lu P. New mechanistic insights into CO2 electroreduction to methane on penta-octa-graphene catalyst. J Energy Chem 2024;99:529–40. https://doi.org/10.1016/j.jechem.2024.08.017.
[120] Verma AM, Kishore N. Efficient CO2 reduction to methane on Ru2-Based adjacent vacant graphene catalysts: insights into bimetallic synergies, thermodynamics, and kinetics. Catal Sci Technol 2025;15(7):2379–94. https://doi.org/10.1039/D5CY00005J.
[121] Cui X, An W, Liu X, Wang H, Men Y, Wang J. C2N-Graphene supported single-atom catalysts for CO2 electrochemical reduction reaction: mechanistic Insight and catalyst screening. Nanoscale 2018;10(32):15262–72. https://doi.org/10.1039/C8NR04961K.
[122] He H, Jagvaral Y. Electrochemical reduction of CO2 on graphene supported transition metals – towards single atom catalysts. Phys Chem Chem Phys 2017;19 (18):11436–46. https://doi.org/10.1039/C7CP00915A.
[123] Han L, Song S, Liu M, Yao S, Liang Z, Cheng H, Ren Z, Liu W, Lin R, Qi G, Liu X, Wu Q, Luo J, Xin HL. Stable and efficient single-atom Zn catalyst for CO2 reduction to CH4. J Am Chem Soc 2020;142(29):12563–7. https://doi.org/10.1021/jacs.9b12111.
[124] Hashiba H, Yotsuhashi S, Deguchi M, Yamada Y. Systematic analysis of electrochemical CO_2 reduction with various reaction parameters using combinatorial reactors. ACS Comb Sci 2016;18(4):203–8. https://doi.org/10.1021/acscombsci.6b00021.
[125] Vos RE, Kolmeijer KE, Jacobs TS, van der Stam W, Weckhuysen BM, Koper MTM. How temperature affects the selectivity of the electrochemical CO2 reduction on copper. ACS Catal 2023;13(12):8080–91. https://doi.org/10.1021/acscatal.3c00706.
[126] Hori Y, Takahashi R, Yoshinami Y, Murata A. Electrochemical reduction of CO at a copper electrode. J Phys Chem B 1997;101(36):7075–81. https://doi.org/10.1021/jp970284i.
[127] Schouten KJP, Pérez Gallent E, Koper MTM. The influence of pH on the reduction of CO and CO 2 to hydrocarbons on copper electrodes. J Electroanal Chem 2014; 716:53–7. https://doi.org/10.1016/j.jelechem.2013.08.033.
[128] Varela AS, Kroschel M, Reier T, Strasser P. Controlling the selectivity of CO2 electroreduction on copper: the effect of the electrolyte concentration and the importance of the local pH. Catal Today 2016;260:8–13. https://doi.org/10.1016/j.cattod.2015.06.009.
[129] Raciti D, Mao M, Park JH, Wang C. Local pH effect in the CO2 reduction reaction on high-surface-area copper electrocatalysts. J Electrochem Soc 2018;165(10): F799. https://doi.org/10.1149/2.0521810jes.
[130] Resasco J, Chen LD, Clark E, Tsai C, Hahn C, Jaramillo TF, Chan K, Bell AT. Promoter effects of alkali metal cations on the electrochemical reduction of carbon dioxide. J Am Chem Soc 2017;139(32):11277–87. https://doi.org/10.1021/jacs.7b06765.
[131] Banerji, L. C.; Jang, H.; Gardner, A. M.; Cowan, A. J. Studying the cation dependence of CO2 reduction intermediates at Cu by in situ VSFG spectroscopy. Chem Sci 15 (8), 2889–2897. https://doi.org/10.1039/d3sc05295h.
[132] El-Nagar GA, Haun F, Gupta S, Stojkovikj S, Mayer MT. Unintended cation crossover influences CO2 reduction selectivity in Cu-Based zero-gap electrolysers. Nat Commun 2023;14(1):2062. https://doi.org/10.1038/s41467-023-37520-x.
[133] Singh MR, Kwon Y, Lum Y, Ager JW, Bell AT. Hydrolysis of electrolyte cations enhances the electrochemical reduction of CO_2 over Ag and Cu. J Am Chem Soc 2016;138(39):13006–12. https://doi.org/10.1021/jacs.6b07612.
[134] Ringe S, Clark EL, Resasco J, Walton A, Seger B, Bell AT, Chan K. Understanding cation effects in electrochemical CO2 reduction. Energy Environ Sci 2019;12(10): 3001–14. https://doi.org/10.1039/C9EE01341E.
[135] Fan M, Miao RK, Ou P, Xu Y, Lin Z-Y, Lee T-J, Hung S-F, Xie K, Huang JE, Ni W, Li J, Zhao Y, Ozden A, O'Brien CP, Chen Y, Xiao YC, Liu S, Wicks J, Wang X, Abed J, Shirzadi E, Sargent EH, Sinton D. Single-Site decorated copper enables Energy- and carbon-efficient CO2 methanation in acidic conditions. Nat Commun 2023;14(1):3314. https://doi.org/10.1038/s41467-023-38935-2.
[136] Pan H, Barile CJ. Electrochemical CO2 reduction to methane with remarkably high faradaic efficiency in the presence of a proton permeable membrane. Energy Environ Sci 2020;13(10):3567–78. https://doi.org/10.1039/D0EE02189J.
[137] Wang X, Xu A, Li F, Hung S-F, Nam D-H, Gabardo CM, Wang Z, Xu Y, Ozden A, Rasouli AS, Ip AH, Sinton D, Sargent EH. Efficient methane electrosynthesis enabled by tuning local CO2 availability. J Am Chem Soc 2020;142(7):3525–31. https://doi.org/10.1021/jacs.9b12445.
[138] Belsa B, Xia L, García de Arquer FP. CO2 electrolysis technologies: bridging the gap toward Scale-up and commercialization. ACS Energy Lett 2024;9(9): 4293–305. https://doi.org/10.1021/acsenergylett.4c00955.
[139] SoCalGas, SoCalGas, PG&E and Opus 12 Announce Advancements in Technology that Converts Carbon Dioxide to Renewable Natural Gas, https://www.socalgas.com/newsroom/press-release/socalgas-pg-e-and-opus-12-announce-advancements-in-technology-that-converts-carbon-dioxide-to-renewable-natural-gas (accessed 2025-10-08).
[140] Xu Z, Lu R, Lin Z-Y, Wu W, Tsai H-J, Lu Q, Li YC, Hung S-F, Song C, Yu JC, Wang Z, Wang Y. Electroreduction of CO2 to methane with triazole molecular catalysts. Nat Energy 2024;9(11):1397–406. https://doi.org/10.1038/s41560-024-01645-0.
[141] Gatti, L.; Verhovez, S.; Mezza, A.; Etzi, M.; Stassi, S.; Pirri, C. F.; Sacco, A. Role of the binder in mitigating salt deposition in 100 Cm2 membrane electrode assembly CO2 electrolyzers. Adv Energy Sustain Res in press, e202500312. https://doi.org/10.1002/aesr.202500312.
[142] Chen S, Su Y, Deng P, Qi R, Zhu J, Chen J, Wang Z, Zhou L, Guo X, Xia BY. Highly selective carbon dioxide electroreduction on structure-evolved copper perovskite oxide toward methane production. ACS Catal 2020;10(8):4640–6. https://doi.org/10.1021/acscatal.0c00847.
[143] Zhao J, Zhang P, Yuan T, Cheng D, Zhen S, Gao H, Wang T, Zhao Z-J, Gong J. Modulation of *CHxO adsorption to facilitate electrocatalytic reduction of CO2 to CH4 over Cu-Based catalysts. J Am Chem Soc 2023;145(12):6622–7. https://doi.org/10.1021/jacs.2c12006.
[144] Xu K, Li J, Liu F, Chen X, Zhao T, Cheng F. Favoring CO intermediate stabilization and protonation by crown ether for CO2 electromethanation in acidic media. Angew Chem Int Ed 2023;62(50):e202311968. https://doi.org/10.1002/anie.202311968.
[145] Chen S, Li W-H, Jiang W, Yang J, Zhu J, Wang L, Ou H, Zhuang Z, Chen M, Sun X, Wang D, Li Y. MOF encapsulating N-Heterocyclic carbene-ligated copper single-atom site catalyst towards efficient methane electrosynthesis. Angew Chem Int Ed 2022;61(4):e202114450. https://doi.org/10.1002/anie.202114450.
[146] Han Z, Han D, Chen Z, Gao J, Jiang G, Wang X, Lyu S, Guo Y, Geng C, Yin L, Weng Z, Yang Q-H. Steering surface reconstruction of copper with electrolyte additives for CO2 electroreduction. Nat Commun 2022;13(1):3158. https://doi.org/10.1038/s41467-022-30819-1.
[147] Chen S, Zhang Z, Jiang W, Zhang S, Zhu J, Wang L, Ou H, Zaman S, Tan L, Zhu P, Zhang E, Jiang P, Su Y, Wang D, Li Y. Engineering water molecules activation Center on multisite electrocatalysts for enhanced CO2 methanation. J Am Chem Soc 2022;144(28):12807–15. https://doi.org/10.1021/jacs.2c03875.
[148] Martín AJ, Larrazábal GO, Pérez-Ramírez J. Towards sustainable fuels and chemicals through the electrochemical reduction of CO2: lessons from water electrolysis. Green Chem 2015;17(12):5114–30. https://doi.org/10.1039/C5GC01893E.
[149] Küngas R. Review—Electrochemical CO2 reduction for CO production: comparison of Low- and high-temperature electrolysis technologies. J Electrochem Soc 2020;167(4):044508. https://doi.org/10.1149/1945-7111/ab7099.
[150] Hawks SA, Ehlinger VM, Moore T, Duoss EB, Beck VA, Weber AZ, Baker SE. Analyzing production rate and carbon utilization trade-offs in CO2RR electrolyzers. ACS Energy Lett 2022;7(8):2685–93. https://doi.org/10.1021/acsenergylett.2c01106.
[151] da Cunha SC, Resasco J. Maximizing single-pass conversion does not result in practical readiness for CO2 reduction electrolyzers. Nat Commun 2023;14(1): 5513. https://doi.org/10.1038/s41467-023-41348-w.
[152] Inoue A, Harada T, Nakanishi S, Kamiya K. Ultra-High-Rate CO 2 reduction reactions to multicarbon products with a Current density of 1.7 A Cm −2 in neutral electrolytes. EES Catal 2023;1(1):9–16. https://doi.org/10.1039/D2EY00035K.

[153] Gattrell M, Gupta N, Co A. Electrochemical reduction of CO2 to hydrocarbons to Store renewable electrical energy and upgrade biogas. Energy Convers Manag 2007;48(4):1255–65. https://doi.org/10.1016/j.enconman.2006.09.019.
[154] Bro R, Smilde AK. Principal component analysis. Anal Methods 2014;6(9): 2812–31. https://doi.org/10.1039/C3AY41907J.
[155] Geladi P, Kowalski BR. Partial least-squares regression: a tutorial. Anal Chim Acta 1986;185:1–17. https://doi.org/10.1016/0003-2670(86)80028-9.
[156] Gabardo CM, O'Brien CP, Edwards JP, McCallum C, Xu Y, Dinh C-T, Li J, Sargent EH, Sinton D. Continuous carbon dioxide electroreduction to concentrated multi-carbon products using a membrane electrode assembly. Joule 2019;3(11):2777–91. https://doi.org/10.1016/j.joule.2019.07.021.
[157] Jouny M, Luc W, Jiao F. General techno-economic analysis of CO2 electrolysis systems. Ind Eng Chem Res 2018;57(6):2165–77. https://doi.org/10.1021/acs.iecr.7b03514.
[158] Bushuyev OS, De Luna P, Dinh CT, Tao L, Saur G, van de Lagemaat J, Kelley SO, Sargent EH. What should we make with CO2 and how can we make it? Joule 2018;2(5):825–32. https://doi.org/10.1016/j.joule.2017.09.003.
[159] Orella MJ, Brown SM, Leonard ME, Román-Leshkov Y, Brushett FR. A general technoeconomic model for evaluating emerging electrolytic processes. Energy Technol 2020;8(11):1900994. https://doi.org/10.1002/ente.201900994.
[160] Wu Y, Du H, Li P, Zhang X, Yin Y, Zhu W. Heterogeneous electrocatalysis of carbon dioxide to methane. Methane 2023;2(2):148–75. https://doi.org/10.3390/methane2020012.
[161] Welch AJ, Digdaya IA, Kent R, Ghougassian P, Atwater HA, Xiang C. Comparative technoeconomic analysis of renewable generation of methane using sunlight, water, and carbon dioxide. ACS Energy Lett 2021;6(4):1540–9. https://doi.org/10.1021/acsenergylett.1c00174.
[162] Natural gas - price - Chart - Historical Data - News. https://tradingeconomics.com/commodity/natural-gas. [Accessed 25 September 2025].
[163] Al-Breiki M, Bicer Y. Techno-Economic evaluation of a power-to-methane plant : levelized cost of methane, financial performance metrics, and sensitivity analysis. Chem Eng J 2023;471:144725. https://doi.org/10.1016/j.cej.2023.144725.
[164] Somoza-Tornos A, Guerra OJ, Crow AM, Smith WA, Hodge B-M. Process modeling, techno-economic assessment, and life cycle assessment of the electrochemical reduction of CO2: a review. iScience 2021;24(7):102813. https://doi.org/10.1016/j.isci.2021.102813.
[165] Jameel MK, Mustafa MA, Ahmed HS, Mohammed AJ, Ghazy H, Shakir MN, Lawas AM, Mohammed SK, Idan AH, Mahmoud ZH, Sayadi H, Kianfar E. Biogas: production, properties, applications, economic and challenges: a review. Results Chem. 2024;7:101549. https://doi.org/10.1016/j.rechem.2024.101549.
[166] Swinbourn R, Li C, Wang F. A comprehensive review on biomethane production from biogas separation and its techno-economic assessments. ChemSusChem 2024;17(19):e202400779. https://doi.org/10.1002/cssc.202400779.
[167] Bagi Z, Ács N, Böjti T, Kakuk B, Rákhely G, Strang O, Szuhaj M, Wirth R, Kovács KL. Biomethane: the energy storage, platform chemical and greenhouse gas mitigation target. Anaerobe 2017;46:13–22. https://doi.org/10.1016/j.anaerobe.2017.03.001.
[168] Paolini V, Tratzi P, Torre M, Tomassetti L, Segreto M, Petracchini F. Chapter 3 - water scrubbing for biogas upgrading: developments and innovations. In: Aryal N, Mørck Ottosen LD, Wegener Kofoed MV, Pant D, editors. Emerging technologies and biological systems for biogas upgrading. Academic Press; 2021. p. 57–71. https://doi.org/10.1016/B978-0-12-822808-1.00001-5.
[169] Han S, Meng Y, Aihemaiti A, Gao Y, Ju T, Xiang H, Jiang J. Biogas upgrading with various single and blended amines solutions: capacities and kinetics. Energy 2022;253:124195. https://doi.org/10.1016/j.energy.2022.124195.
[170] Ali Abd A, Roslee Othman M, Helwani Z, Kim J. An overview of biogas upgrading via pressure swing adsorption: navigating through bibliometric insights towards a conceptual framework and future research pathways. Energy Convers Manag 2024;306:118268. https://doi.org/10.1016/j.enconman.2024.118268.
[171] Naquash A, Qyyum MA, Haider J, Bokhari A, Lim H, Lee M. State-of-the-Art assessment of cryogenic technologies for biogas upgrading: energy, economic, and environmental perspectives. Renew Sustain Energy Rev 2022;154:111826. https://doi.org/10.1016/j.rser.2021.111826.
[172] Aguilloso G, Arpia K, Khan M, Sapico ZA, Lopez ECR. Recent advances in membrane technologies for biogas upgrading. Eng Proc 2024;67(1):57. https://doi.org/10.3390/engproc2024067057.
[173] Wu L, Wei W, Song L, Woźniak-Karczewska M, Chrzanowski Ł, Ni B-J. Upgrading biogas produced in anaerobic digestion: biological removal and bioconversion of CO2 in biogas. Renew Sustain Energy Rev 2021;150:111448. https://doi.org/10.1016/j.rser.2021.111448.
[174] Wegener Kofoed MV, Jensen MB, Mørck Ottosen LD. Biological upgrading of biogas through CO2 conversion to CH4. In: Aryal N, Mørck Ottosen LD, Wegener Kofoed MV, Pant D, editors. Emerging technologies and biological systems for biogas upgrading. Academic Press; 2021. p. 321–62. https://doi.org/10.1016/B978-0-12-822808-1.00012-X.
[175] Stangeland K, Kalai D, Li H, Yu Z. CO2 methanation: the effect of catalysts and reaction conditions. Energy Proc 2017;105:2022–7. https://doi.org/10.1016/j.egypro.2017.03.577.
[176] Wei J, Gu Y, Wu X. Modeling and comparison of typical design of filter-press flow electrochemical reactors. Ind Eng Chem Res 2022;61(9):3303–19. https://doi.org/10.1021/acs.iecr.2c00280.
[177] Mahant B, Linga P, Kumar R. Hydrogen economy and role of hythane as a bridging solution: a perspective review. Energy Fuels 2021;35(19):15424–54. https://doi.org/10.1021/acs.energyfuels.1c02404.
[178] Huang Z, Lu L, Jiang D, Xing D, Ren ZJ. Electrochemical hythane production for renewable energy storage and biogas upgrading. Appl Energy 2017;187:595–600. https://doi.org/10.1016/j.apenergy.2016.11.099.
[179] Mohammadpour H, Pivrikas A, Cheng KY, Ho G. A three-chamber electrochemical cell facilitated biogas upgrading and high-purity oxygen production. J Appl Electrochem 2022;52(6):919–27. https://doi.org/10.1007/s10800-022-01680-3.
[180] Liu C, Sun D, Zhao Z, Dang Y, Holmes DE. *Methanothrix* enhances biogas upgrading in microbial electrolysis cell via direct electron transfer. Bioresour Technol 2019;291:121877. https://doi.org/10.1016/j.biortech.2019.121877.
[181] Liu C, Xiao J, Li H, Chen Q, Sun D, Cheng X, Li P, Dang Y, Smith JA, Holmes DE. High efficiency *in-Situ* biogas upgrading in a bioelectrochemical System with low energy input. Water Res 2021;197:117055. https://doi.org/10.1016/j.watres.2021.117055.
[182] Acosta N, Sakarika M, Kerckhof F-M, Law CKY, De Vrieze J, Rabaey K. Microbial protein production from methane *via* electrochemical biogas upgrading. Chem Eng J 2020;391:123625. https://doi.org/10.1016/j.cej.2019.123625.
[183] Makaryan IA, Sedov IV, Salgansky EA, Arutyunov AV, Arutyunov VS. A comprehensive review on the prospects of using hydrogen–methane blends: challenges and opportunities. Energies 2022;15(6):2265. https://doi.org/10.3390/en15062265.